

Impact of Phase-Shift Error on the Secrecy Performance of Uplink RIS Communication Systems

Abdelhamid Salem, *Member, IEEE*, Kai-Kit Wong, *Fellow, IEEE*, and Chan-Byoung Chae,

Fellow, IEEE

Abstract

Reconfigurable intelligent surface (RIS) has been recognized as a promising technique for the sixth generation (6G) of mobile communication networks. The key feature of RIS is to reconfigure the propagation environment via smart signal reflections. In addition, active RIS schemes have been recently proposed to overcome the deep path loss attenuation inherent in the RIS-aided communication systems. Accordingly, this paper considers the secrecy performance of up-link RIS-aided multiple users multiple-input single-output (MU-MISO) communication systems, in the presence of multiple passive eavesdroppers. In contrast to the existing works, we investigate the impact of the RIS phase shift errors on the secrecy performance. Taking into account the complex environment, where a general Rician channel model is adopted for all the communication links, closed-form approximate expressions for the ergodic secrecy rate are derived for three RIS configurations, namely, i) passive RIS, ii) active RIS, iii) active RIS with energy harvesting (EH RIS). Then, based on the derived expressions, we optimize the phase shifts at the RIS to enhance the system performance. In addition, the best RIS configuration selection is considered for a given target secrecy rate and amount of the power available at the users. Finally, Monte-Carlo simulations are provided to verify the accuracy of the analysis, and the impact of different system parameters on the secrecy performance is investigated. The results in this

Abdelhamid Salem is with the department of Electronic and Electrical Engineering, University College London, London, UK, (emails: a.salem@ucl.ac.uk).

Kai-Kit Wong is with the department of Electronic and Electrical Engineering, University College London, London, UK, Kai-Kit Wong is also affiliated with Yonsei University, Seoul, Korea (email: kai-kit.wong@ucl.ac.uk).

Chan-Byoung Chae is with Yonsei University, Seoul, Korea (e-mail: cbchae@yonsei.ac.kr).

The work is supported by the Engineering and Physical Sciences Research Council (EPSRC) under grant EP/V052942/1. For the purpose of open access, the authors will apply a Creative Commons Attribution (CCBY) licence to any Author Accepted Manuscript version arising.

paper show that, an active RIS scheme can be implemented to enhance the secrecy performance of RIS-aided communication systems with phase shift errors, especially when the users have limited transmission power.

Index Terms

Reconfigurable intelligent surface, Physical layer security, MU-MISO, MRC.

I. INTRODUCTION

Reconfigurable intelligent surface (RIS), also known as intelligent reflecting surface (IRS), has been proposed recently as a promising technique to extend the coverage and improve the spectral efficiency of wireless communication networks [1], [2]. Specifically, RIS is composed of reflecting elements, each of which independently imposes a phase shift on the incident signals. By tuning the phase shifts of the reflecting elements, RIS can convert the propagation environments into smart ones and thus enhance the received signals quality [1], [2]. Due to these advantages, RIS techniques have been extensively considered in the literature. For instance, in [3], the fundamental capacity limit of RIS-aided multiple-input multipleoutput (MIMO) communication systems has been considered. The achievable ergodic rate of a RIS-assisted MIMO system which comprises links of a Rician channel was derived in [4]. In [5], a closed-form asymptotic ergodic sum rate of a RIS-assisted MIMO communication system was derived under the assumption that the number of base station (BS) antennas tends to infinity. In [6], the up-link achievable rate in RIS-aided massive MIMO systems has been analyzed and optimized. The authors in [7], [8] analyzed the achievable rate of RIS-assisted multiple users (MU) up-link massive MIMO system under Rician fading channels. In [9], [10], a closed-form expression of ergodic achievable rate for RIS-aided massive MIMO systems with zero forcing (ZF) detector has been derived. In addition, a closed-form analytical expression for the symbol error probability and the upper bound on the channel capacity of a RIS communication system have been derived in [11]. The work in [12] considered the impact of hardware impairments on a general RIS MU-MISO system with Rayleigh fading channels. The ergodic capacity of RIS MIMO networks over Rayleigh-Rician channels was considered in [13].

However, the practical implementation of passive RIS-aided communication systems may face several challenges. For instance, the transmitted signal propagates through the RIS experiences a double-fading attenuation, e.g, source-RIS and RIS-destination links. This issue has been tackled in the literature by increasing the number of passive RIS elements [14]. However, this solution leads to an increase in

the size of the RIS module, which is impractical in some scenarios. To tackle this issue the authors in [15] proposed RIS with active elements. The main idea of active RIS is to adjust the phase shifts and also amplify the reflected signal attenuated from the first link with extra power consumption. Theoretical comparison between the active RIS-assisted system and the passive RIS-aided system has been presented in [16]. The results in [16] show that the active RIS has better performance than passive RIS. The use of active RIS elements to overcome the double-fading problem has been also investigated in [17], where the results illustrated that using active elements results in a severe reduction in the physical size of RIS to achieve a certain performance. To reduce the power consumption of active RIS, a sub-connected architecture has been proposed in [18]. The energy efficiency in an active RIS-aided MU-MISO down-link system has been investigated in [19].

Although fixed embedded batteries can be used to power the RIS, these batteries cannot be relied on for long time and uninterrupted operations. In addition, wired charging might not be possible to use if the RIS is deployed in inaccessible places. Therefore, equipping RIS elements with energy harvesting (EH) modules can solve these issues. Accordingly, a self-sustainable RIS approach was proposed and studied in the recent researches on RIS. In this regard, in [20] time switching (TS) and power splitting (PS) EH protocols for the RIS to harvest sufficient amount of energy from an access point have been proposed and investigated. The work in [21] considered a self-sustainable RIS-aided MU-MISO communication systems, in which the RIS collected energy from the radio frequency (RF) transmitter using the PS protocol. In [22], a novel transmission policy for a communication network assisted by self-sustainable RIS has been proposed, where the RIS harvests energy from an energy transmitter to support its operation. In [23], self-sustainable RIS with the PS protocol to assist broadcasting network was studied. In [24], self-sustainable RIS-aided communication between a gateway and a device was studied, in which the RIS harvested energy prior communication.

Moreover, due to the broadcast nature of wireless channels, confidential messages are vulnerable to eavesdropping attacks. For the provision of secure transmission, physical layer security (PHYSec) has been proposed from the information theory perspective [25], [26]. PHYSec exploits the nature of wireless channels to enhance the system security [25], [26]. PHYSec of RIS systems has also been studied in the literature. In [27], the secrecy throughput maximization problem has been formulated and solved to enhance the secrecy performance of the RIS-assisted MIMO systems. In [28], a novel active RIS design to enhance the security of wireless transmission was proposed. PHYSec of RIS-

aided wireless networks has been considered in [29] to achieve secure transmission between a source and a legitimate user in the presence of a malicious eavesdropper. In [30], RIS has been used to perform secure transmission from a multiple antennas transmitter to a multiple antennas legitimate receiver. Further work in [31] considered the secrecy transmission in a RIS-aided multiple antennas communication, where the secrecy rate was improved by optimizing the RIS location. In [32], an active RIS-aided multiple antennas PHYSec transmission scheme was considered, where the active RIS was designed to amplify the signal actively.

Accordingly, this paper investigates the impact of phase shift error on the secrecy performance of up-link RIS-aided MU-MISO systems in the presence of multiple eavesdroppers. The BS receives the users messages only through the RIS, while eavesdroppers can receive the signals from both the direct and reflected links. Under Rician fading channels and phase shift errors, the ergodic secrecy rate is analyzed for three RIS configurations, namely, 1) passive RIS, 2) active RIS, and 3) EH RIS. Based on the derived rate expressions, the phase shifts at the RIS are optimized to enhance the system performance. Then, the best RIS configuration selection is considered based on the target secrecy rate and amount of power available at the users. For clarity we list the main contributions of this work as follows:

- 1) We investigate the impact of RIS phase shift error on the secrecy performance of up-link MU-MIMO systems in the presence of multiple passive eavesdroppers.
- 2) New closed-form explicit analytical expressions for the ergodic secrecy rate are derived for the RIS-assisted MU-MIMO systems, when the RIS is passive, active and EH node under Rician fading channels. This channel model is more general but also very challenging to be considered mathematically. The derived secrecy rate expressions are simple, explicit and in closed form, and provide several important practical design insights.
- 3) Based on the derived expressions, a genetic algorithm (GA)-based approach is used to obtain the optimal phase shifts. Also, a simple suboptimal technique is proposed to enhance the secrecy rate for a legitimate user.
- 4) Given a target secrecy rate, we calculate the required user power, and we present steps to select best RIS configuration which depend mainly on the available power at the users.
- 5) Finally, Monte-Carlo simulations are performed to validate the analytical expressions. Then, the impact of several system parameters on the secrecy performance are investigated.

The results in this work show that active RIS is an efficient scheme to achieve secure communication in the presence of phase shift errors at the RIS, especially when there is no sufficient amount of power at the users.

Next, Section II presents the RIS-aided uplink MU-MISO system model. In Section III, we derive the ergodic secrecy rate of the passive RIS model. Section IV presents the ergodic secrecy rate of the active RIS scheme. Section V derives the ergodic secrecy rate of the EH RIS scheme. Section VII depicts our numerical results. Our main conclusions are summarized in Section VIII.

II. SYSTEM MODEL

Consider a typical up-link RIS-aided MU-MISO communication system consisting of a multiple antennas BS, an RIS and K single-antenna users in the presence of J single antenna passive eavesdroppers. The BS is equipped with N antennas, and the RIS is equipped with M reflecting elements, as shown in Fig. 1.

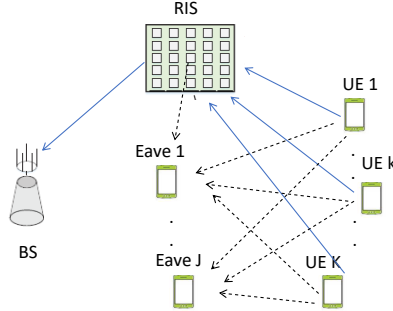


Figure 1: An RIS-aided uplink MU-MISO system with N BS antennas, M RIS elements, K users and J eavesdroppers.

The BS and RIS are connected to control and adjust the phase shifts of the the RIS elements. It is assumed that the eavesdroppers can hear the signals from the direct and reflected links, and trying to eavesdrop a specific confidential message in the system. On the other side, the direct links between the users and BS are assumed to be blocked, which justifies the use of the RIS. It is known that, the RIS is most likely to be installed on the buildings, and thus it can create channels dominated by line-of-sight (LoS) path along with scatters. Accordingly, a Rician fading model is considered for the RIS channels. The channel matrix between the RIS and the BS is denoted by $\mathbf{G} \in \mathbb{C}^{N \times M}$, and the channel vector

between user k and the RIS is presented by $\mathbf{h}_{r,k} \in C^{M \times 1}$. The mathematical expressions of the channel matrix \mathbf{G} and the channel vector $\mathbf{h}_{r,k}$ can be expressed, respectively, as

$$\mathbf{G} = \left(\sqrt{\frac{\rho_b}{\rho_b + 1}} \bar{\mathbf{G}} + \sqrt{\frac{1}{\rho_b + 1}} \tilde{\mathbf{G}} \right), \quad \mathbf{h}_{r,k} = \left(\sqrt{\frac{\rho_k}{\rho_k + 1}} \bar{\mathbf{h}}_{r,k} + \sqrt{\frac{1}{\rho_k + 1}} \tilde{\mathbf{h}}_{r,k} \right) \quad (1)$$

where ρ_b and ρ_k are the Rician factors, $\bar{\mathbf{G}}$ and $\bar{\mathbf{h}}_{r,k}$ are the LoS components and $\tilde{\mathbf{G}}$ and $\tilde{\mathbf{h}}_{r,k}$ are the NLoS components, in which

$$\bar{\mathbf{G}} = \mathbf{a}_N(\phi_r^a, \phi_r^e) \mathbf{a}_M^H(\phi_t^a, \phi_t^e), \quad \bar{\mathbf{h}}_{r,k} = \mathbf{a}_M(\phi_{kr}^a, \phi_{kr}^e) \quad (2)$$

where ϕ_{kr}^a, ϕ_{kr}^e denote the azimuth and elevation angles of arrival (AoA) from user k to the RIS, respectively, ϕ_t^a, ϕ_t^e are the azimuth and elevation angles of departure (AoD) at the BS from the RIS, respectively, ϕ_r^a, ϕ_r^e are the azimuth and elevation AoA from the RIS to the BS, respectively. The k th element of the vector \mathbf{a}_X can be written as $[\mathbf{a}_X(\phi_1, \phi_2)]_k = e^{j2\pi \frac{d}{\lambda}(x_k \sin \phi_1 \sin \phi_2 + y_k \cos \phi_2)}$, where λ is the wavelength, d is the elements/antennas spacing, and $x_k = (k-1) \bmod \sqrt{X}$, $y_k = \frac{k-1}{\sqrt{X}}$. On the other hand, the channel vector between the RIS and eavesdropper j is presented by $\mathbf{h}_{e_j,r} \in C^{1 \times M}$, and the channel from user k to eavesdropper j is $h_{e_j,k} \in C^{1 \times 1}$. The direct channel fading is assumed to be Rayleigh fading due to extensive scatterers, while for the RIS-related channels, is assumed to be Rician fading. Thus the expression of $\mathbf{h}_{e_j,r}$ is given by

$$\mathbf{h}_{e_j,r} = \left(\sqrt{\frac{\rho_{e_j,r}}{\rho_{e_j,r} + 1}} \bar{\mathbf{h}}_{e_j,r} + \sqrt{\frac{1}{\rho_{e_j,r} + 1}} \tilde{\mathbf{h}}_{e_j,r} \right) \quad (3)$$

where $\rho_{e_j,r}$ is the Rician factor, $\bar{\mathbf{h}}_{e_j,r}$ and $\tilde{\mathbf{h}}_{e_j,r}$ are the LoS of NLoS components, respectively.

The channel state information (CSI) of the eavesdroppers is assumed to be unknown at the BS/RIS (only statistical information can be known), and the eavesdroppers are non-colluding. Therefore, the ergodic secrecy rate can be calculated by [33]

$$\hat{R}_s = \left[\hat{R}_{b_k} - \hat{R}_{e_{j,k}} \right]^+ \quad (4)$$

where $[l]^+ = \max(0, l)$, $\hat{R}_{b_k} = \mathcal{E}\{R_{b_k}\}$, R_{b_k} is the up-link rate of user k , and $\hat{R}_{e_{j,k}} = \max \mathcal{E}\{R_{e_{j,k}}\}$, $R_{e_{j,k}}$ is the rate at eavesdropper j .

In the following sections, we consider the secrecy performance of the three RIS configurations.

III. PASSIVE RIS

As we have mentioned earlier, passive RIS reflects the users messages constructively to the BS with passive elements. Thus, the received signal at the BS can be expressed as

$$\mathbf{y}_b = \sum_{k=1}^K \sqrt{p_k L_{u_k,b}} \mathbf{G} \tilde{\Theta} \mathbf{h}_{r,k} x_k + \mathbf{n}_b \quad (5)$$

where $L_{u_k,b} = d_{u_k,r}^{-\alpha_r} d_{r,b}^{-\alpha_b}$ is the large scale fading, $d_{u_k,r}$ is the distance between user k and RIS, $d_{r,b}$ is the distance between RIS and the BS, α_r and α_b are the path-loss exponents, \mathbf{n}_b is the additive wight Gaussian noise (AWGN) at the BS, $\mathbf{n}_b \sim CN(0, \sigma_b^2 \mathbf{I})$, $\tilde{\Theta} = \bar{\Theta} \Theta$ where $\Theta = \text{diag}(\theta)$, and $\theta = [\theta_1, \dots, \theta_M]^T$ is the RIS reflection coefficients with $\theta_m = e^{j\varphi_m}$, where $\varphi_m \in [0, 2\pi)$ is the phase shift of element m . However, in practical systems, phase shift errors can exist due to imperfect channel knowledge and finite precision in phase adjustment. Thus, we define $\bar{\Theta} = [e^{j\bar{\varphi}_1}, \dots, e^{j\bar{\varphi}_M}]$ as the phase-shift errors at the RIS. The phase-error is modeled according to Von-Mises (VM) distribution with zero-mean and a characteristic function (CF) $E[e^{j\bar{\varphi}_m}] = \frac{I_1(\kappa)}{I_0(\kappa)} = \rho(\kappa)$, where κ is the concentration parameter and I_i is the modified Bessel function of the first kind and order i . By applying the receive beamforming vector \mathbf{w}_k at the BS, the received signal of user k is

$$\mathbf{y}_{b,k} = \sqrt{p_k L_{u_k,b}} \mathbf{w}_k \mathbf{G} \bar{\Theta} \Theta \mathbf{h}_{r,k} x_k + \sum_{\substack{i=1 \\ i \neq k}}^K \sqrt{p_i L_{u_i,b}} \mathbf{w}_k \mathbf{G} \bar{\Theta} \Theta \mathbf{h}_{r,i} x_i + \mathbf{w}_k \mathbf{n}_b. \quad (6)$$

On the other hand, the received signal at eavesdropper j to detect user k signal is

$$\begin{aligned} y_{e_j,k} = & \sqrt{p_k} x_k \left(\sqrt{d_{e_j,k}^{-\alpha_e}} h_{e_j,k} + \sqrt{L_{u_k,e_j}} \mathbf{h}_{e_j,r} \bar{\Theta} \Theta \mathbf{h}_{r,k} \right) \\ & + \sum_{\substack{i=1 \\ i \neq k}}^K \sqrt{p_i} x_i \left(\sqrt{d_{e_j,i}^{-\alpha_e}} h_{e_j,i} + \sum_{\substack{i=1 \\ i \neq k}}^K \sqrt{L_{u_i,e_j}} \mathbf{h}_{e_j,r} \bar{\Theta} \Theta \mathbf{h}_{r,i} \right) + n_{e_j} \end{aligned} \quad (7)$$

where $d_{e_j,k}^{-\alpha_e}$ is the distance between user k and eavesdropper j , α_e is the path-loss exponent, $L_{u_k,B} = d_{u_k,r}^{-\alpha_r} d_{r,b}^{-\alpha_b}$ and $d_{e_j,r}^{-\alpha_e}$ denotes the distance between the RIS and eavesdropper j .

To calculate the ergodic secrecy rate, the ergodic up-link rate for user k and ergodic rate at the eavesdropper j should be derived, which will be considered in the following sub-sections.

A. Ergodic Up-link rate of user k

To calculate the ergodic user rate, maximum ratio combining (MRC) is adopted at the BS. The beamforming matrix is given by $\mathbf{W} = (\mathbf{G}\Theta\mathbf{H})^H$, and thus $\mathbf{w}_k = \mathbf{h}_{r,k}^H \Theta^H \mathbf{G}^H$. The signal to interference plus noise ratio (SINR) at the BS to decode user k signal can be written as

$$\gamma_{b_k} = \frac{p_k L_{u_k,b} |\mathbf{h}_{r,k}^H \Theta^H \mathbf{G}^H \mathbf{G} \Theta \bar{\mathbf{h}}_{r,k}|^2}{\sum_{\substack{i=1 \\ i \neq k}}^K p_i L_{u_i,b} |\mathbf{h}_{r,k}^H \Theta^H \mathbf{G}^H \mathbf{G} \Theta \bar{\mathbf{h}}_{r,i}|^2 + \|\mathbf{h}_{r,k}^H \Theta^H \mathbf{G}^H\|^2 \sigma_b^2}. \quad (8)$$

Lemma 1. *The ergodic up-link rate of user k in passive RIS-aided MU-MISO systems under Rician fading channels and with phase shift error can be calculated by*

$$\mathcal{E} \{R_{b_k}\} \approx \log_2 \left(1 + \frac{p_k L_{u_k,b} \xi_k}{\sum_{\substack{i=1 \\ i \neq k}}^K p_i L_{u_i,b} \varsigma_i + v_k \sigma_b^2} \right) \quad (9)$$

where

$$\xi_k = \mathcal{E} \left\{ |\mathbf{h}_{r,k}^H \Theta^H \mathbf{G}^H \mathbf{G} \Theta \bar{\mathbf{h}}_{r,k}|^2 \right\} = \frac{1}{(\rho_b + 1)^2 (\rho_k + 1)^2} (a_1 N^2 + a_2 N M^2 + a_3 N M + a_4 N)$$

$$\begin{aligned} a_1 &= (\rho(\kappa)^2 (\rho_k + \rho_b + 1)^2 + (1 - \rho(\kappa)^2) \rho_k \rho_b^2 + \rho_b^2) M^2 \\ &+ ((2\rho_k + 3\rho_b + 2 - \rho_k \rho_b) \rho(\kappa)^2 + (1 + \rho_k) \rho_b) \rho_b \rho_k |f_k|^2 + (\rho_k + \rho_b + 2)^2 \\ &- \rho(\kappa)^2 (\rho_k + \rho_b + 1)^2 - 2\rho(\kappa)^2 \rho_k \rho_b - 2) M \\ &+ \rho(\kappa)^2 \rho_b^2 \rho_k^2 |f_k|^4 + 2((1 - \rho(\kappa)^2) (\rho_k + \rho_b) + 2) \rho_b \rho_k |f_k|^2, \\ a_2 &= (-\rho(\kappa)^2 \rho_k \rho_b (1 + \rho_k) M^2) + (\rho_k + \rho_b + 1) \rho_b \rho_r + (\rho_k + \rho_b + 1)^2 - (\rho_k + 1) \rho_b^2, \\ a_3 &= (((\rho_k + 1) \rho(\kappa)^2) + (\rho_k + 1)) \rho_b \rho_k |f_k|^2 - 2\rho_b \rho_k \rho(\kappa)^2 + 2\rho_b \rho_k + 2\rho_k + 2\rho_b - 1, \\ a_4 &= 2\rho_b \rho_r |f_k|^2 (1 + \rho(\kappa)^2) \end{aligned}$$

and

$$\varsigma_i = \mathcal{E} \left\{ \left| \mathbf{h}_{r,k}^H \Theta^H \mathbf{G}^H \mathbf{G} \Theta \bar{\mathbf{h}}_{r,i} \right|^2 \right\} = \frac{1}{(\rho_b + 1)^2 (\rho_k + 1) (\rho_i + 1)} (b_1 N^2 + b_2 N M^2 + b_3 N M)$$

$$\begin{aligned} b_1 &= (\rho_i + 1 - \rho(\kappa)^2 \rho_i) M^2 \rho_b^2 \\ &+ M \left((\rho_i + 1 - \rho(\kappa)^2 \rho_i) \rho_b^2 \rho_k |f_k|^2 + \rho(\kappa)^2 \rho_b^2 \rho_i |f_i|^2 + (\rho_k + 2\rho_b + 1) (\rho_i + 1 - \rho(\kappa)^2 \rho_i) + \rho(\kappa)^2 \rho_i \right) \\ &+ \left(2\rho_b |f_i|^2 + \rho_k |\bar{\mathbf{h}}_k^H \bar{\mathbf{h}}_i|^2 + 2\rho_b \rho_k \text{Re} (f_k^* f_i \bar{\mathbf{h}}_i^H \bar{\mathbf{h}}_k) \right) \rho(\kappa)^2 \rho_i \\ &+ (\rho(\kappa)^2 \rho_b \rho_i |f_i|^2 + 2\rho_i (1 - \rho(\kappa)^2) + 2) \rho_b \rho_k |f_k|^2 \\ b_2 &= ((\rho_b + 1) \rho_k + (\rho_b + 1)^2 - \rho_b^2) (\rho_i + 1) - (\rho_b + 1) \rho_b \rho_i \rho(\kappa)^2 - 1 \\ b_3 &= (\rho_i + 1) \rho_b \rho_k |f_k|^2 + (\rho_k + 1) \rho(\kappa)^2 \rho_b \rho_i |f_i|^2 \end{aligned}$$

and

$$v_k = \mathcal{E} \left\{ \left\| \mathbf{h}_{r,k}^H \Theta^H \mathbf{G}^H \right\|^2 \right\} = \frac{L_{u_k,b}}{(\rho_b + 1) (\rho_k + 1)} (\rho_b \rho_k |f_k|^2 + (\rho_b + \rho_k + 1) M)$$

Proof: The proof is provided in Appendix A. ■

B. Ergodic Rate at Eavesdropper j

The SINR at eavesdropper j to decode user k signal can be expressed as

$$\gamma_{e_j,k} = \frac{p_k \left| d_{u_k,r}^{-\frac{\alpha_r}{2}} d_{e_j,r}^{-\frac{\alpha_e}{2}} \mathbf{h}_{e_j,r} \Theta \bar{\mathbf{h}}_{r,k} + d_{e_j,k}^{-\frac{\alpha_e}{2}} h_{e_j,k} \right|^2}{\sum_{\substack{i=1 \\ i \neq k}}^K p_i \left| d_{u_i,r}^{-\frac{\alpha_r}{2}} d_{e_j,r}^{-\frac{\alpha_e}{2}} \mathbf{h}_{e_j,r} \Theta \bar{\mathbf{h}}_{r,i} + d_{e_j,i}^{-\frac{\alpha_e}{2}} h_{e_j,i} \right|^2 + \sigma_{e_j}^2}. \quad (10)$$

Lemma 2. *The ergodic rate at eavesdropper j in up-link passive RIS-aided MU-MISO systems under Rician fading channels and with phase shift error can be calculated by*

$$\mathcal{E} \{ R_{e_j,k} \} = \log_2 \left(1 + \frac{p_k x_k}{\sum_{\substack{i=1 \\ i \neq k}}^K p_i y_i + \sigma_{e_j}^2} \right) \quad (11)$$

where

$$x_k = \left(d_{u_k,r}^{-\alpha_r} d_{e_j,r}^{-\alpha_e} \left(\frac{\rho_{e_j}}{\rho_{e_j} + 1} \frac{\rho_k}{\rho_k + 1} (M + \rho(\kappa)^2 \xi) + \frac{\rho_{e_j}}{\rho_{e_j} + 1} \frac{1}{\rho_k + 1} M + \frac{\rho_k}{\rho_k + 1} \frac{1}{\rho_{e_j} + 1} M + \frac{1}{\rho_{e_j} + 1} \frac{1}{\rho_k + 1} M \right) + d_{e_j,r}^{-\alpha_e} \right),$$

and

$$y_i = d_{u_i,r}^{-\alpha_r} d_{e_j,r}^{-\alpha_e} \left(\frac{\rho_{e_j}}{\rho_{e_j}+1} \frac{\rho_i}{\rho_i+1} (M + \rho(\kappa)^2 \xi) + \frac{\rho_{e_j}}{\rho_{e_j}+1} \frac{1}{\rho_i+1} M + \frac{\rho_i}{\rho_i+1} \frac{1}{\rho_{e_j}+1} M + \frac{1}{\rho_{e_j}+1} \frac{1}{\rho_i+1} M + d_{e_j,i}^{-\alpha_e} \right).$$

Proof: The proof is provided in Appendix B. ■

Finally, the ergodic secrecy rate in passive RIS scheme is presented in the next theorem.

Theorem 1. *The ergodic secrecy rate in passive RIS-aided MU-MISO systems under Rician fading channels and with phase shift error can be calculated by*

$$\hat{R}_s = \left[\log_2 \left(1 + \frac{p_k L_{u_k,b} \xi_k}{\sum_{\substack{i=1 \\ i \neq k}}^K p_i L_{u_i,b} \varsigma_i + v_k \sigma_b^2} \right) - \log_2 \left(1 + \frac{p_k x_k}{\sum_{\substack{i=1 \\ i \neq k}}^K p_i y_i + \sigma_{e_j}^2} \right) \right]. \quad (12)$$

IV. ACTIVE RIS

As we mentioned earlier, active RIS can adjust the phase shifts and also amplify the reflected signal to compensate the attenuation from the first link with extra power consumption. The signal reflected by the active IRS can be written as

$$\mathbf{y}_r = \tilde{\Theta} \sum_{k=1}^K \sqrt{p_k d_{u_k,r}^{-\alpha_r}} \mathbf{h}_{r,i} x_i + \tilde{\Theta} \mathbf{n}_r \quad (13)$$

where \mathbf{n}_r is the noise at RIS elements $\mathbf{n}_r \sim \mathcal{CN}(0, \sigma_r^2 \mathbf{I})$. In this case $\tilde{\Theta} = \bar{\Theta} \Theta$ where $\Theta = \text{diag}(\theta)$, and $\theta = [\theta_1, \dots, \theta_M]^T$ with $\theta_m = \varrho_m e^{j\varphi_m}$, $\varrho_m > 1$ and $\varphi_m \in [0, 2\pi)$ represents the amplification factor and phase shift coefficient, respectively, at element m . For simplicity, we assume that $\varrho_m = \varrho$ and then define $\Theta = \varrho \text{diag}\{e^{j\varphi_1}, \dots, e^{j\varphi_M}\}$. The active RIS amplification power can be expressed as

$$P_r = \left(\sum_{k=1}^K \frac{p_k}{d_{u_k,r}^{\alpha_r}} \mathcal{E} \left\{ \left\| \tilde{\Theta} \mathbf{h}_{r,i} \right\|^2 \right\} + \mathcal{E} \left\{ \left\| \tilde{\Theta} \mathbf{n}_r \right\|^2 \right\} \right) = \left(\sum_{k=1}^K \frac{p_k}{d_{u_k,r}^{\alpha_r}} M \varrho^2 + M \varrho^2 \sigma_r^2 \right) \quad (14)$$

where $\mathcal{E} \left\| \tilde{\Theta} \mathbf{n}_r \right\|^2 = M \varrho^2 \sigma_r^2$, and $\mathcal{E} \left\| \tilde{\Theta} \mathbf{h}_{r,i} \right\|^2 = \frac{\varrho^2}{\rho_i+1} \left(\rho_i \mathcal{E} \left(\bar{\mathbf{h}}_{r,i}^H \bar{\mathbf{h}}_{r,i} \right) + \mathcal{E} \left(\tilde{\mathbf{h}}_{r,i}^H \tilde{\mathbf{h}}_{r,i} \right) \right) = \frac{\varrho^2}{\rho_i+1} (\rho_i M + M) = M \varrho^2$. Thus, the amplification factor for each element on the active RIS is given by

$$\varrho = \sqrt{\frac{P_r}{M \left(\sum_{k=1}^K \frac{p_k}{d_{u_k,r}^{\alpha_r}} + \sigma_r^2 \right)}}. \quad (15)$$

By applying the receive beamforming vector \mathbf{w}_k at the BS, the received signal of user k is

$$y_{b,k} = \sqrt{p_k L_{u_k,b}} \mathbf{w}_k^H \mathbf{G} \bar{\Theta} \Theta \mathbf{h}_{r,k} x_k + \sum_{\substack{i=1 \\ i \neq k}}^K \sqrt{p_i L_{u_i,b}} \mathbf{w}_k^H \mathbf{G} \bar{\Theta} \Theta \mathbf{h}_{r,i} x_i + \sqrt{d_{r,b}^{-\alpha_r}} \mathbf{w}_k^H \mathbf{G} \bar{\Theta} \Theta \mathbf{n}_r + \mathbf{w}_k^H \mathbf{n}_b. \quad (16)$$

On the other hand, the received signal at eavesdropper j to detect user k signal is

$$y_{e_j,k} = \sqrt{p_k} x_k \left(\sqrt{d_{e_j,k}^{-\alpha_e}} h_{e_j,k} + \sqrt{L_{u_k,e_j}} \mathbf{h}_{e_j,r}^H \bar{\Theta} \Theta \mathbf{h}_{r,k} \right) + \sum_{\substack{i=1 \\ i \neq k}}^K \sqrt{p_i} x_i \left(\sqrt{d_{e_j,i}^{-\alpha_e}} h_{e_j,i} + \sum_{\substack{i=1 \\ i \neq k}}^K \sqrt{L_{u_i,e_j}} \mathbf{h}_{e_j,r}^H \bar{\Theta} \Theta \mathbf{h}_{r,i} \right) + \sqrt{d_{e_j,r}^{-\alpha_e}} \mathbf{h}_{e_j,r}^H \bar{\Theta} \Theta \mathbf{n}_r + n_{e_j}. \quad (17)$$

A. Ergodic Up-link rate of user k

Applying MRC beamforming at the BS, the SINRs at the BS to decode user k signal can be expressed as

$$\gamma_{b_k} = \frac{p_k L_{u_k,b} \left| \mathbf{h}_{r,k}^H \Theta^H \mathbf{G}^H \mathbf{G} \bar{\Theta} \Theta \mathbf{h}_{r,k} \right|^2}{\sum_{\substack{i=1 \\ i \neq k}}^K p_i L_{u_i,b} \left| \mathbf{h}_{r,k}^H \Theta^H \mathbf{G}^H \mathbf{G} \bar{\Theta} \Theta \mathbf{h}_{r,i} \right|^2 + d_{r,b}^{-\alpha_r} \left\| \mathbf{h}_{r,k}^H \Theta^H \mathbf{G}^H \mathbf{G} \bar{\Theta} \Theta \right\|^2 \sigma_r^2 + \left\| \mathbf{h}_{r,k}^H \Theta^H \mathbf{G}^H \right\|^2 \sigma_b^2}. \quad (18)$$

Lemma 3. *The ergodic up-link rate of user k in active RIS-aided MU-MISO systems under Rician fading channels and with phase shift error can be calculated by*

$$\mathcal{E} \{R_{b_k}\} \approx \log_2 \left(1 + \frac{p_k L_{u_k,b} \xi_k \varrho^4}{\sum_{\substack{i=1 \\ i \neq k}}^K p_i L_{u_i,b} \varsigma_i \varrho^4 + \varrho^4 d_{r,b}^{-\alpha_r} \sigma_r^2 \nu_k + \varrho^2 \nu_k \sigma_b^2} \right) \quad (19)$$

where

$$\nu_k = \mathcal{E} \left\| \mathbf{h}_{r,k}^H \Theta^H \mathbf{G}^H \mathbf{G} \bar{\Theta} \Theta \right\|^2 = \frac{1}{(\rho_b + 1) \sqrt{(\rho_k + 1)}} (X_1 + X_2) \quad (20)$$

and $X_1 = \mathcal{E} \{|\Delta_{1,1}|^2\} + \mathcal{E} \{|\Delta_{1,2}|^2\} + \mathcal{E} \{|\Delta_{1,3}|^2\} + \mathcal{E} \{|\Delta_{1,4}|^2\} + \mathcal{E} \{\Delta_{1,1} \Delta_{1,4}^*\}$

$$\mathcal{E} \{ |\Delta_{1,1}|^2 \} = \rho_b^2 \rho_k \left| \left(a_M^H(\phi_{kr}^a, \phi_{kr}^e) \Theta^H a_M^H(\phi_r^a, \phi_r^e) a_N^H(\phi_b^a, \phi_b^e) a_N(\phi_b^a, \phi_b^e) \right) \right|^2 \times M,$$

$$\mathcal{E} \{ |\Delta_{1,2}|^2 \} = \rho_b \rho_k \left| a_M^H(\phi_{kr}^a, \phi_{kr}^e) \Theta^H a_M(\phi_r^a, \phi_r^e) \right|^2 N M,$$

$$\mathcal{E} \{ |\Delta_{1,3}|^2 \} = \rho_b \rho_k M N \left(\rho(\kappa)^2 M + (1 - \rho(\kappa)^2) M \right), \quad \mathcal{E} \{ |\Delta_{1,4}|^2 \} = \rho_k (N^2 M + N M^2),$$

$$\mathcal{E} \{ \Delta_{1,1} \Delta_{1,4}^* \} = \rho_b \rho_k \left(a_M^H(\phi_{kr}^a, \phi_{kr}^e) \Theta^H a_M^H(\phi_r^a, \phi_r^e) a_N^H(\phi_b^a, \phi_b^e) a_N(\phi_b^a, \phi_b^e) \right)$$

$$\times \left(a_M(\phi_r^a, \phi_r^e) \Theta \right) \rho_k a_M^H(\phi_{kr}^a, \phi_{kr}^e) \Theta^H N \Theta,$$

$$\text{and } X_2 = \mathcal{E} \{ |\Delta_{2,1}|^2 \} + \mathcal{E} \{ |\Delta_{2,2}|^2 \} + \mathcal{E} \{ |\Delta_{2,3}|^2 \} + \mathcal{E} \{ |\Delta_{2,4}|^2 \} + \mathcal{E} \{ \Delta_{2,1} \Delta_{2,4}^* \}$$

$$\mathcal{E} \{ |\Delta_{2,1}|^2 \} = \rho_b^2 \left\| \Theta^H a_M^H(\phi_r^a, \phi_r^e) a_N^H(\phi_b^a, \phi_b^e) a_N(\phi_b^a, \phi_b^e) a_M(\phi_r^a, \phi_r^e) \Theta \right\|_F^2,$$

$$\mathcal{E} \{ |\Delta_{2,2}|^2 \} = \rho_b \left\| \Theta^H a_M(\phi_r^a, \phi_r^e) \right\|^2 N M,$$

$$\mathcal{E} \{ |\Delta_{2,3}|^2 \} = \rho_b M N \left(\left\| a_M^H(\phi_r^a, \phi_r^e) \Theta \bar{\Theta} \right\|^2 \right) = \rho_b M^2 N, \quad \mathcal{E} \{ |\Delta_{2,4}|^2 \} = \rho_k^2 (N^2 M + N M^2),$$

$$\mathcal{E} \{ \Delta_{2,1} \Delta_{2,4}^* \} = \rho_k \left(\Theta^H a_M^H(\phi_r^a, \phi_r^e) a_N^H(\phi_b^a, \phi_b^e) a_N(\phi_b^a, \phi_b^e) \right) \left(a_M(\phi_r^a, \phi_r^e) \Theta \right) \rho_k \Theta N \Theta^H.$$

Proof: The proof is provided in Appendix C. ■

B. Ergodic Rate at Eavesdropper j

The SINR at eavesdropper j to decode user k signal in this scenario can be written as

$$\gamma_{e,j,k} = \frac{p_k \left| d_{u_k,r}^{-\frac{\alpha_r}{2}} d_{e_j,r}^{-\frac{\alpha_e}{2}} \mathbf{h}_{e_j,r} \Theta \bar{\Theta} \mathbf{h}_{r,k} + d_{e_j,k}^{-\frac{\alpha_e}{2}} h_{e_j,k} \right|^2}{\sum_{\substack{i=1 \\ i \neq k}}^K p_i \left| d_{u_i,r}^{-\frac{\alpha_r}{2}} d_{e_j,r}^{-\frac{\alpha_e}{2}} \mathbf{h}_{e_j,r} \Theta \bar{\Theta} \mathbf{h}_{r,i} + d_{e_j,i}^{-\frac{\alpha_e}{2}} h_{e_j,i} \right|^2 + d_{e_j,r}^{-\alpha_e} \|\mathbf{h}_{e_j,r} \bar{\Theta} \Theta\|^2 \sigma_r^2 + \sigma_{e_j}^2}. \quad (21)$$

Lemma 4. *The ergodic rate at eavesdropper j in up-link active RIS-aided MU-MISO systems under Rician fading channels and with phase shift error can be calculated by*

$$\mathcal{E} \{ R_{e,j,k} \} = \log_2 \left(1 + \frac{p_k x_j}{\sum_{\substack{i=1 \\ i \neq k}}^K p_i y_i + z_j \sigma_r^2 + \sigma_{e_j}^2} \right) \quad (22)$$

where

$$x_j = \left(d_{u_k,r}^{-\alpha_r} d_{e_j,r}^{-\alpha_e} \varrho^2 \left(\frac{\rho_{e_j}}{\rho_{e_j}+1} \frac{\rho_k}{\rho_k+1} (M + \rho(\kappa)^2 \xi) + \frac{\rho_{e_j}}{\rho_{e_j}+1} \frac{1}{\rho_k+1} M + \frac{\rho_k}{\rho_k+1} \frac{1}{\rho_{e_j}+1} M + \frac{1}{\rho_{e_j}+1} \frac{1}{\rho_k+1} M \right) + d_{e_j,r}^{-\alpha_e} \right),$$

$$y_k = d_{u_i,r}^{-\alpha_r} d_{e_j,r}^{-\alpha_e} \varrho^2 \left(\frac{\rho_{e_j}}{\rho_{e_j}+1} \frac{\rho_i}{\rho_i+1} (M + \rho(\kappa)^2 \xi) + \frac{\rho_{e_j}}{\rho_{e_j}+1} \frac{1}{\rho_i+1} M + \frac{\rho_i}{\rho_i+1} \frac{1}{\rho_{e_j}+1} M + \frac{1}{\rho_{e_j}+1} \frac{1}{\rho_i+1} M + d_{e_j,i}^{-\alpha_e} \right)$$

which have been derived in Appemdix B, and

$$z_j = d_{e_j,r}^{-\alpha_e} \mathcal{E} \left\| \mathbf{h}_{e_j,r} \tilde{\Theta} \right\|^2 = d_{e_j,r}^{-\alpha_e} \frac{\varrho^2}{\rho_{e_j,r}+1} \left(\rho_{e_j,r} \mathcal{E} \left(\bar{\mathbf{h}}_{e_j,r}^H \bar{\mathbf{h}}_{e_j,r} \right) + \mathcal{E} \left(\tilde{\mathbf{h}}_{e_j,r}^H \tilde{\mathbf{h}}_{e_j,r} \right) \right)$$

$$= d_{e_j,r}^{-\alpha_e} \frac{\varrho^2}{\rho_{e_j,r}+1} (\rho_{e_j,r} M + M) = d_{e_j,r}^{-\alpha_e} M \varrho^2.$$

The ergodic secrecy rate in active RIS scheme is presented in the following Theorem.

Theorem 2. *The ergodic secrecy rate in active RIS-aided MU-MISO systems under Rician fading channels and with phase shift error can be calculated by*

$$\hat{R}_s = \left[\log_2 \left(1 + \frac{p_k L_{u_k,b} \xi_k \varrho^4}{\sum_{\substack{i=1 \\ i \neq k}}^K p_i L_{u_i,b} \varsigma_i \varrho^4 + \varrho^4 d_{r,b}^{-\alpha_r} \sigma_r^2 \nu_k + \varrho^2 \nu_k \sigma_b^2} \right) - \log_2 \left(1 + \frac{p_k x_j}{\sum_{\substack{i=1 \\ i \neq k}}^K p_i y_i + z_j \sigma_r^2 + \sigma_{e_j}^2} \right) \right]^+. \quad (23)$$

V. EH RIS

Following the recent works in [20], [21], [22], [23], [24], in this section, the RIS is an energy constrained node and it can harvest RF energy to support its operation. Thus, in this scenario the

whole operation time block, T , is split into two time periods, the energy transfer (ET) slot and the information transfer (IT) slot. During the ET slot, the BS transmits energy signals to the RIS to support its operation. During the IT slot, the users deliver their messages to the BS through the RIS. We denote τT as the time duration for the ET, and $(1 - \tau) T$ as the time duration for IT. The received signals at the RIS in the first sub-slot is expressed as

$$y_r = \sqrt{P_b} \mathbf{G}_p \mathbf{W}_p \mathbf{x}_p + \mathbf{n}_r \quad (24)$$

where P_b is the BS power, $\mathbf{G}_p = \left(\sqrt{\frac{\rho_p}{\rho_p+1}} \bar{\mathbf{G}}_p + \sqrt{\frac{1}{\rho_p+1}} \tilde{\mathbf{G}}_p \right)$ is the BS-RIS channel in the ET slot, \mathbf{W}_p is the precoding matrix and \mathbf{x}_p is the energy signals vector. Using the maximum ratio transmission (MRT) scheme, the harvested power at the RIS can be expressed as $P_r = \frac{\eta_{eff} \tau P_b \|\mathbf{G}_p\|_F^2}{1-\tau}$, which can be written as $P_r = \frac{\eta_{eff} \tau P_b \text{Tr}(\mathbf{G}_b \mathbf{G}_b^H)}{1-\tau}$ where η_{eff} is the efficiency of EH. Since $\mathbf{G}_b \mathbf{G}_b^H$ has Wishart distribution, the average harvested power can be written as

$$P_r = \frac{\eta_{eff} \tau P_b \mathcal{E} \{ \text{Tr}(\mathbf{G}_b \mathbf{G}_b^H) \}}{1-\tau} = \frac{\eta_{eff} \tau P_b N M}{1-\tau}. \quad (25)$$

By substituting (25) into (15), the amplification factor for each element on the RIS in this case is given by

$$\hat{\varrho} = \sqrt{\frac{\eta_{eff} \tau P_b N M}{M (1-\tau) \left(\sum_{k=1}^K \frac{p_k}{d_{u_k,r}^{\alpha_r}} + \sigma_r^2 \right)}}. \quad (26)$$

A. Ergodic Up-link rate of user k

Applying MRC beamforming at the BS, the SINR at the BS to decode user k signal can be expressed as

$$\gamma_{b_k} = \frac{p_k L_{u_k,b} \left| \mathbf{h}_{r,k}^H \Theta^H \mathbf{G}^H \mathbf{G} \Theta \bar{\Theta} \mathbf{h}_{r,k} \right|^2}{\sum_{\substack{i=1 \\ i \neq k}}^K p_i L_{u_i,b} \left| \mathbf{h}_{r,k}^H \Theta^H \mathbf{G}^H \mathbf{G} \Theta \bar{\Theta} \mathbf{h}_{r,i} \right|^2 + d_{r,b}^{-\alpha_r} \left\| \mathbf{h}_{r,k}^H \Theta^H \mathbf{G}^H \mathbf{G} \bar{\Theta} \Theta \right\|^2 \sigma_r^2 + \left\| \mathbf{h}_{r,k}^H \Theta^H \mathbf{G}^H \right\|^2 \sigma_b^2}. \quad (27)$$

Lemma 5. *The ergodic up-link rate of user k in EH RIS-aided MU-MISO systems under Rician fading channels and with phase shift error can be calculated by*

$$\mathcal{E} \{R_{b_k}\} \approx (1 - \tau) \log_2 \left(1 + \frac{p_k L_{u_k,b} \xi_k \hat{\varrho}^4}{\sum_{\substack{i=1 \\ i \neq k}}^K p_i L_{u_i,b} \varsigma_i \hat{\varrho}^4 + \hat{\varrho}^4 d_{r,b}^{-\alpha_r} \sigma_r^2 \nu_k + \hat{\varrho}^2 \nu_k \sigma_b^2} \right). \quad (28)$$

Proof: This expression can be obtained by following same derivation in Appendix C. ■

B. Ergodic Rate at Eavesdropper j

The SINR at eavesdropper j to decode user k signal is given by

$$\gamma_{e_j,k} = \frac{p_k \left| d_{u_k,r}^{-\frac{\alpha_r}{2}} d_{e_j,r}^{-\frac{\alpha_e}{2}} \mathbf{h}_{e_j,r} \Theta \bar{\Theta} \mathbf{h}_{r,k} + d_{e_j,k}^{-\frac{\alpha_e}{2}} h_{e_j,k} \right|^2}{\sum_{\substack{i=1 \\ i \neq k}}^K p_i \left| d_{u_i,r}^{-\frac{\alpha_r}{2}} d_{e_j,r}^{-\frac{\alpha_e}{2}} \mathbf{h}_{e_j,r} \Theta \bar{\Theta} \mathbf{h}_{r,i} + d_{e_j,i}^{-\frac{\alpha_e}{2}} h_{e_j,i} \right|^2 + d_{e_j,r}^{-\alpha_e} \|\mathbf{h}_{e_j,r} \bar{\Theta} \Theta\|^2 \sigma_r^2 + \sigma_{e_j}^2}. \quad (29)$$

Lemma 6. *The ergodic rate at eavesdropper j in up-link EH RIS-aided MU-MISO systems under Rician fading channels and with phase shift error can be calculated by*

$$\mathcal{E} \{R_{e_j,k}\} = (1 - \tau) \log_2 \left(1 + \frac{p_k \hat{x}_j}{\sum_{\substack{i=1 \\ i \neq k}}^K p_i \hat{y}_i + \hat{z}_j \sigma_r^2 + \sigma_{e_j}^2} \right) \quad (30)$$

where

$$\begin{aligned} \hat{x}_j &= \left(d_{u_k,r}^{-\alpha_r} d_{e_j,r}^{-\alpha_e} \hat{\varrho}^2 \left(\frac{\rho_{e_j}}{\rho_{e_j}+1} \frac{\rho_k}{\rho_k+1} (M + \rho(\kappa)^2 \xi) + \frac{\rho_{e_j}}{\rho_{e_j}+1} \frac{1}{\rho_k+1} M + \frac{\rho_k}{\rho_k+1} \frac{1}{\rho_{e_j}+1} M + \frac{1}{\rho_{e_j}+1} \frac{1}{\rho_k+1} M \right) + d_{e_j,r}^{-\alpha_e} \right), \\ \hat{y}_i &= d_{u_i,r}^{-\alpha_r} d_{e_j,r}^{-\alpha_e} \hat{\varrho}^2 \left(\frac{\rho_{e_j}}{\rho_{e_j}+1} \frac{\rho_i}{\rho_i+1} (M + \rho(\kappa)^2 \xi) + \frac{\rho_{e_j}}{\rho_{e_j}+1} \frac{1}{\rho_i+1} M + \frac{\rho_i}{\rho_i+1} \frac{1}{\rho_{e_j}+1} M + \frac{1}{\rho_{e_j}+1} \frac{1}{\rho_i+1} M + d_{e_j,i}^{-\alpha_e} \right) \\ \hat{z}_j &= d_{e_j,r}^{-\alpha_e} M \hat{\varrho}^2, \end{aligned}$$

which have been derived in the previous section.

Finally, the ergodic secrecy rate in EH RIS scheme is presented in the next Theorem.

Theorem 3. *The ergodic secrecy rate of user k in EH active RIS-aided MU-MISO systems under Rician fading channels and with phase shift error can be calculated by*

$$\hat{R}_s = \left[(1 - \tau) \log_2 \left(1 + \frac{p_k L_{u_k,b} \xi_k \hat{\varrho}^4}{\sum_{\substack{i=1 \\ i \neq k}}^K p_i L_{u_i,b} \varsigma_i \hat{\varrho}^4 + \hat{\varrho}^4 d_{r,b}^{-\alpha_r} \sigma_r^2 \nu_k + \hat{\varrho}^2 \nu_k \sigma_b^2} \right) - (1 - \tau) \log_2 \left(1 + \frac{p_k \hat{x}_j}{\sum_{\substack{i=1 \\ i \neq k}}^K p_i \hat{y}_i + \hat{z}_j \sigma_r^2 + \sigma_{e_j}^2} \right) \right]^+ . \quad (31)$$

VI. SYSTEM DESIGN

In this section, based on the derived analytical expressions, we first design the phase shifts of the RIS configurations considered in this work. Then, the best RIS configuration selection scheme is presented.

A. Phase Shift Optimization

The secrecy rate expressions presented in Theorems, 1, 2 and 3, show that the secrecy performance relies on the phase shifts of the RIS elements. In this work, it is assumed that the CSI of the eavesdroppers is unknown at the BS/RIS (only channel distribution known). Therefore, to enhance the system performance, the RIS phase shifts can be optimized by maximizing the achievable ergodic sum rate. Since the phase shift at each unit of the RIS lies in the range of $[0; 2\pi)$, the phase shift optimization problem can be formulated as

$$\begin{aligned} \max_{\Theta} \quad & \sum_{i=1}^K \hat{R}_{b_i} \\ \text{s.t.} \quad & \theta_m \in [0, 2\pi), \quad \forall m. \end{aligned} \quad (32)$$

Due to the complicated formula of the ergodic sum rate, it is difficult to optimize (32) based on the conventional techniques. However, GA-based methods can be employed to solve this optimization problem. Due to the page limitation, we refer readers to [6] for more details about the GA methods.

As an efficient suboptimal solution, the RIS phase shifts can be aligned to user k , who transmits the confidential message. This presents a simple sub-optimal solution for enhancing the secrecy rate [6]. Accordingly, the phase shifts should be

$$\theta_m = -2\pi \frac{d}{\lambda} (x_m t_k + y_m l_k), \quad t_k = \sin \phi_{kr}^a \sin \phi_{kr}^e - \sin \phi_t^a \sin \phi_t^e, \quad l_k = \cos \phi_{kr}^e - \cos \phi_t^e. \quad (33)$$

B. RIS Configuration Selection Scheme

Based on the required secrecy rate (r_s) and amount of the power available at user k , and the RIS, we can decide which system configuration, i.e., passive RIS, active RIS or EH RIS, should be selected.

A) If user k has sufficient amount of power to achieve the target secrecy rate, in this case passive RIS can be implemented. Based on the secrecy rate expression provided in Theorem 1, the required user k power, p_k , to achieve the target secrecy rate, r_s , can be obtained by solving

$$r_s = \log_2 \left(1 + \frac{p_k L_{u_k, b} \xi_k}{\sum_{\substack{i=1 \\ i \neq k}}^K p_i L_{u_i, b} \varsigma_i + v_k \sigma_b^2} \right) - \log_2 \left(1 + \frac{p_k x_k}{\sum_{\substack{i=1 \\ i \neq k}}^K p_i y_i + \sigma_{e_j}^2} \right) \quad (34)$$

which can be found as

$$p_k = \frac{p_1 - p_2}{p_3 - p_4} \quad (35)$$

$$\text{where } p_1 = \frac{\sum_{\substack{i=1 \\ i \neq k}}^K p_i L_{u_i, b} \varsigma_i + v_k \sigma_b^2}{\sum_{\substack{i=1 \\ i \neq k}}^K p_i L_{u_i, b} \varsigma_i + v_k \sigma_b^2}, \quad p_2 = \frac{2^{r_s} \sum_{\substack{i=1 \\ i \neq k}}^K p_i y_i + 2^{r_s} \sigma_{e_j}^2}{\sum_{\substack{i=1 \\ i \neq k}}^K p_i y_i + \sigma_{e_j}^2}, \quad p_3 = \frac{2^{r_s} x_k}{\sum_{\substack{i=1 \\ i \neq k}}^K p_i y_i + \sigma_{e_j}^2} \text{ and } p_4 = \frac{L_{u_k, b} \xi_k}{\sum_{\substack{i=1 \\ i \neq k}}^K p_i L_{u_i, b} \varsigma_i + v_k \sigma_b^2}.$$

B) If user k has limited amount of power, e.g., the user power, p_k , is less than the power required in (35). In this case active RIS can be implemented to provide the target secrecy rate. Based on the secrecy rate expression provided in Theorem 2, the required RIS power, ϱ or P_r , to achieve the target secrecy rate, r_s , can be obtained by solving

$$\begin{aligned}
r_s = \log_2 & \left(1 + \frac{p_k L_{u_k,b} \xi_k \varrho^2}{\sum_{\substack{i=1 \\ i \neq k}}^K p_i L_{u_i,b} \varsigma_i \varrho^2 + \varrho^2 d_{r,b}^{-\alpha_r} \sigma_r^2 \nu_k + v_k \sigma_b^2} \right) \\
& - \log_2 \left(1 + \frac{p_k \varrho^2 x_1 + p_k x_2}{\sum_{\substack{i=1 \\ i \neq k}}^K p_i \varrho^2 y_{1i} + \sum_{\substack{i=1 \\ i \neq k}}^K p_i y_{2i} + z_1 \varrho^2 \sigma_r^2 + \sigma_{e_j}^2} \right)
\end{aligned} \tag{36}$$

where $x_1 = d_{u_k,r}^{-\alpha_r} d_{e_j,r}^{-\alpha_e} \left(\frac{\rho_{e_j}}{\rho_{e_j}+1} \frac{\rho_k}{\rho_k+1} (M + \rho(\kappa)^2 \xi) + \frac{\rho_{e_j}}{\rho_{e_j}+1} \frac{1}{\rho_k+1} M + \frac{\rho_k}{\rho_k+1} \frac{1}{\rho_{e_j}+1} M + \frac{1}{\rho_{e_j}+1} \frac{1}{\rho_k+1} M \right)$, $x_2 = d_{e_j,r}^{-\alpha_e}$,
 $y_{1i} = d_{u_i,r}^{-\alpha_r} d_{e_j,r}^{-\alpha_e} \left(\frac{\rho_{e_j}}{\rho_{e_j}+1} \frac{\rho_i}{\rho_i+1} (M + \rho(\kappa)^2 \xi) + \frac{\rho_{e_j}}{\rho_{e_j}+1} \frac{1}{\rho_i+1} M + \frac{\rho_i}{\rho_i+1} \frac{1}{\rho_{e_j}+1} M + \frac{1}{\rho_{e_j}+1} \frac{1}{\rho_i+1} M \right)$, $y_{2i} = d_{e_j,i}^{-\alpha_e}$,
and $z_1 = d_{e_j,r}^{-\alpha_e} M$. After some simplifications, the last equation can be expressed as

$$\varrho^4 (q_1 - q_3) + \varrho^2 (q_2 - q_4 - q_5 + q_7) + (q_8 - q_6) = 0 \tag{37}$$

where

$$\begin{aligned}
q_1 &= \sum_{\substack{i=1 \\ i \neq k}}^K p_i L_{u_i,b} \varsigma_i \sum_{\substack{i=1 \\ i \neq k}}^K p_i y_{1i} + d_{r,b}^{-\alpha_r} \sigma_r^2 \nu_k \sum_{\substack{i=1 \\ i \neq k}}^K p_i y_{1i} + \sum_{\substack{i=1 \\ i \neq k}}^K p_i L_{u_i,b} \varsigma_i z_1 \sigma_r^2 + d_{r,b}^{-\alpha_r} \sigma_r^2 \nu_k z_1 \sigma_r^2 + \sum_{\substack{i=1 \\ i \neq k}}^K p_i L_{u_i,b} \varsigma_i p_k x_1 + \\
& d_{r,b}^{-\alpha_r} \sigma_r^2 \nu_k p_k x_1, \\
q_2 &= \left(v_k \sigma_b^2 \sum_{\substack{i=1 \\ i \neq k}}^K p_i y_{1i} + v_k \sigma_b^2 z_1 \sigma_r^2 + v_k \sigma_b^2 p_k x_1 \right), \\
q_3 &= \sum_{\substack{i=1 \\ i \neq k}}^K p_i y_{1i} p_k L_{u_k,b} \xi_k + z_1 \sigma_r^2 p_k L_{u_k,b} \xi_k + \sum_{\substack{i=1 \\ i \neq k}}^K p_i y_{1i} \sum_{\substack{i=1 \\ i \neq k}}^K p_i L_{u_i,b} \varsigma_i + z_1 \sigma_r^2 \sum_{\substack{i=1 \\ i \neq k}}^K p_i L_{u_i,b} \varsigma_i + \sum_{\substack{i=1 \\ i \neq k}}^K p_i y_{1i} d_{r,b}^{-\alpha_r} \sigma_r^2 \nu_k + \\
& z_1 \sigma_r^2 d_{r,b}^{-\alpha_r} \sigma_r^2 \nu_k, \\
q_4 &= \sum_{\substack{i=1 \\ i \neq k}}^K p_i y_{2i} p_k L_{u_k,b} \xi_k + \sigma_{e_j}^2 p_k L_{u_k,b} \xi_k + \sum_{\substack{i=1 \\ i \neq k}}^K p_i y_{2i} \sum_{\substack{i=1 \\ i \neq k}}^K p_i L_{u_i,b} \varsigma_i + \sigma_{e_j}^2 \sum_{\substack{i=1 \\ i \neq k}}^K p_i L_{u_i,b} \varsigma_i + \sum_{\substack{i=1 \\ i \neq k}}^K p_i y_{2i} d_{r,b}^{-\alpha_r} \sigma_r^2 \nu_k + \\
& \sigma_{e_j}^2 d_{r,b}^{-\alpha_r} \sigma_r^2 \nu_k, \\
q_5 &= \left(\sum_{\substack{i=1 \\ i \neq k}}^K p_i y_{1i} v_k \sigma_b^2 + z_1 \sigma_r^2 v_k \sigma_b^2 \right), \quad q_6 = \sum_{\substack{i=1 \\ i \neq k}}^K p_i y_{2i} v_k \sigma_b^2 + \sigma_{e_j}^2 v_k \sigma_b^2, \\
q_7 &= \sum_{\substack{i=1 \\ i \neq k}}^K p_i L_{u_i,b} \varsigma_i \varrho^2 2^{r_s} p_k x_2 + \varrho^2 d_{r,b}^{-\alpha_r} \sigma_r^2 \nu_k 2^{r_s} p_k x_2 + \sum_{\substack{i=1 \\ i \neq k}}^K p_i L_{u_i,b} \varsigma_i 2^{r_s} \sigma_{e_j}^2 + d_{r,b}^{-\alpha_r} \sigma_r^2 \nu_k 2^{r_s} \sigma_{e_j}^2 + \sum_{\substack{i=1 \\ i \neq k}}^K p_i L_{u_i,b} \varsigma_i 2^{r_s} \sum_{\substack{i=1 \\ i \neq k}}^K \\
& p_i y_{2i} + d_{r,b}^{-\alpha_r} \sigma_r^2 \nu_k 2^{r_s} \sum_{\substack{i=1 \\ i \neq k}}^K p_i y_{2i},
\end{aligned}$$

$$q_8 = v_k \sigma_b^2 2^{r_s} p_k x_2 + v_k \sigma_b^2 2^{r_s} \sigma_{e_j}^2 + v_k \sigma_b^2 2^{r_s} \sum_{\substack{i=1 \\ i \neq k}}^K p_i y_{2i}.$$

Thus, from (15), the RIS power should be higher than or equal to

$$P_r = M \left(\frac{-(q_2 - q_4 - q_5 + q_7) \pm \sqrt{(q_2 - q_4 - q_5 + q_7)^2 - 4(q_1 - q_3)(q_8 - q_6)}}{2(q_1 - q_3)} \right) \left(\sum_{k=1}^K \frac{p_k}{d_{u_k, r}^{\alpha_r}} + \sigma_r^2 \right). \quad (38)$$

C) If user k and the RIS have limited amount of power, e.g., user k power, p_k , is less than the required power in (35) and the RIS power, P_r , is less than the required power in (38). In this case EH RIS can be implemented to provide the target secrecy rate. Based on (25) and (38), the required BS power, P_b , to charge the RIS and achieve the target secrecy rate, r_s , can be obtained by

$$P_b = \frac{M(1-\tau)}{\eta_{eff} \tau N M} \left(\frac{-(q_2 - q_4 - q_5 + q_7) \pm \sqrt{(q_2 - q_4 - q_5 + q_7)^2 - 4(q_1 - q_3)(q_8 - q_6)}}{2(q_1 - q_3)} \right) \times \left(\sum_{k=1}^K \frac{p_k}{d_{u_k, r}^{\alpha_r}} + \sigma_r^2 \right). \quad (39)$$

VII. NUMERICAL RESULTS

In this section, we present simulation and numerical results to assess the accuracy of the derived expressions and the secrecy performance of the RIS schemes considered in this paper. Monte-Carlo simulations with 10^5 independent trials are executed. The locations of the BS and the RIS are (0 m, 0 m), (20 m, 20 m), respectively, while the users are scattered on the corners of a square. Specifically, the coordinates for the users square are (30 m, 5 m), (35 m, 5 m), (30 m, -5 m), and (35 m, -5 m), respectively, while the eavesdroppers are distributed in a circle centered at (20 m, 0 m) with radius of 10 m. Unless otherwise specified, the simulation settings are assumed as follows: $K = J = 4$, $N = 10$, $M = 5$, the users power $p_i = 2$ W, the active RIS power $P_r = 7$ W, the BS power in EH RIS scenario $P_b = 50$ W, and the nodes have same noise variance, $\sigma^2 = -70$ dBm. In addition, the path-loss exponent is 2.7, the Rician factors $\rho = 0.5$. The values of the AoA and AoD of the BS and the RIS are uni-formally distributed in $(0, 2\pi)$, and the concentration parameter of RIS phase error $\kappa = 2$.

Firstly, in Fig. 2, we illustrate the ergodic secrecy rate versus the transmission user power, p_k , for the three considered RIS schemes. Fig. 2a shows the secrecy rate with phase shift errors and Fig. 2b, presents the secrecy rate for the ideal scenario, when there is no phase error at RIS. It is clear from this figure that the analytical results are in good agreement with the simulated results, which confirms the validity of the analysis presented in this paper. It is also evident that for the given parameters values, the secrecy rate loss due to the imperfect phase shift at the RIS is about 0.75 bits/s/Hz. In addition, passive RIS achieves the lowest secrecy rate, but with small amount of power consumption. The secrecy rate gain of active RIS above passive RIS is about 0.8 bits/s/Hz for a given user power. Furthermore, high secrecy rates can be achieved and controlled by implementing EH RIS. However, in this case the BS should transmit high power in the EH phase to provide sufficient amount of energy at the RIS to achieve higher secrecy rates.

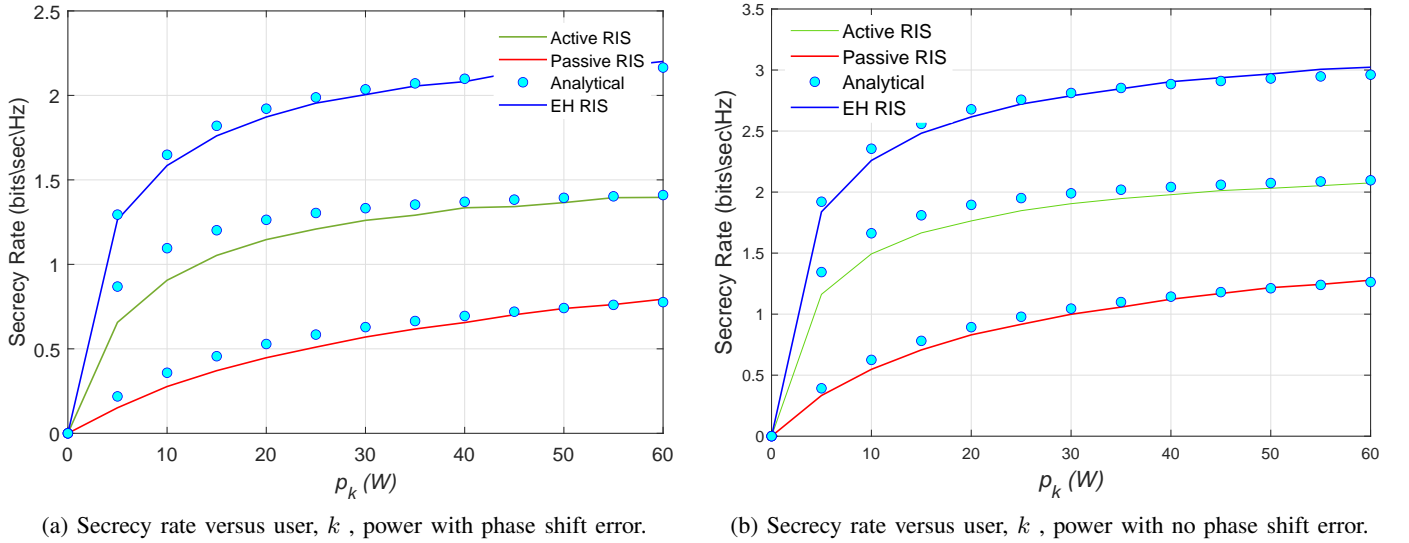


Figure 2: Secrecy rate versus user, k , power with and without phase shift error.

To explain the impact of the phase errors at the RIS on the secrecy performance, in Fig. 3, we plot the secrecy rate versus the concentration parameter of the phase error, κ . Additionally, the results of ideal RIS are also presented in this figure. It can be observed from these results that the secrecy rate enhances as the concentration parameter, κ , increases. In addition, at high concentration parameter values, $\kappa \rightarrow \infty$, the secrecy rate achieved by imperfect RIS saturates to that achieved by ideal RIS. This can be explained by the fact that the phase error at the RIS is assumed to follow a Von Mises distribution, thus high concentration parameter values make the error fluctuate in a smaller range, and

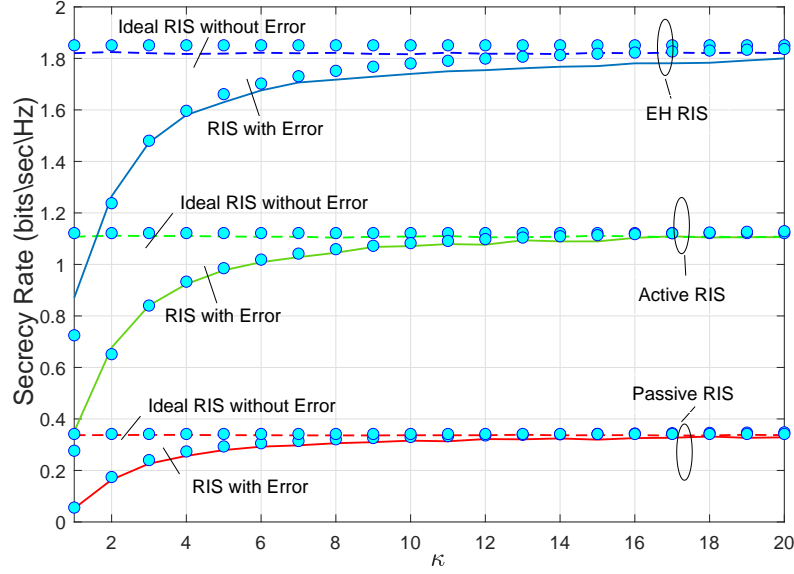


Figure 3: Secrecy rate versus concentration parameter, κ , of RIS phase error.

when $\kappa \rightarrow \infty$, the error at the RIS tends to zero. Accordingly, the secrecy rate of imperfect RIS converges to the ideal RIS case as $\kappa \rightarrow \infty$, as explained in Fig. 3.

Furthermore, Fig. 4 shows the secrecy rate versus the number of BS antennas N for the all RIS schemes. It is evident and as expected, increasing the number of BS antennas N enhances the secrecy performance for the all RIS schemes. It should be pointed out that the number of BS antennas, N , has impact only on the received signal at the BS, thus increasing N results in enhancing the rate of the legitimate users. However N dose not have any impact on the rate at the eavesdroppers. Having said that in EH RIS, increasing N also increases the amount of the harvested energy at the RIS. Thus, in EH RIS, N has impact on both achievable rates at the BS and the eavesdroppers.

In Fig. 5, we depict the secrecy rate versus the number of RIS elements, M , for the all considered RIS schemes. To obtain clear insights and results, in this figure the noise variance at the nodes is assumed to be $\sigma^2 = -20$ dBm. Notably and as expected, increasing M results in enhancing the secrecy rate for the all considered scenarios. In addition, as we can notice from the analytical expressions of the secrecy rate presented in this paper, the number of RIS elements M has impact on both the achievable rate at the BS and the eavesdroppers, e.g., adding more RIS elements increases the rate at the BS and the eavesdroppers. However this improvement in the rate is essential at the BS, because the RIS phase shifts are designed to be toward the BS direction. Furthermore, in the EH RIS scheme, increasing the

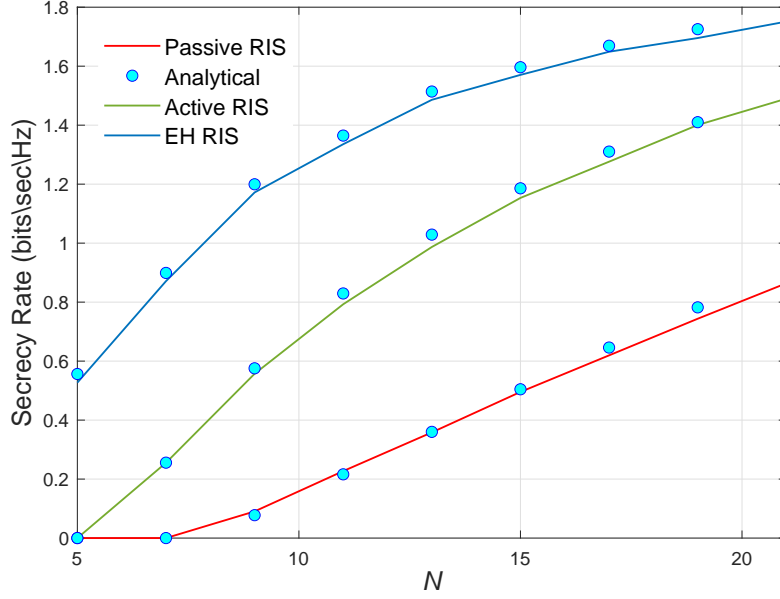


Figure 4: Secrecy rate versus number of BS antennas, N , with phase shift error.

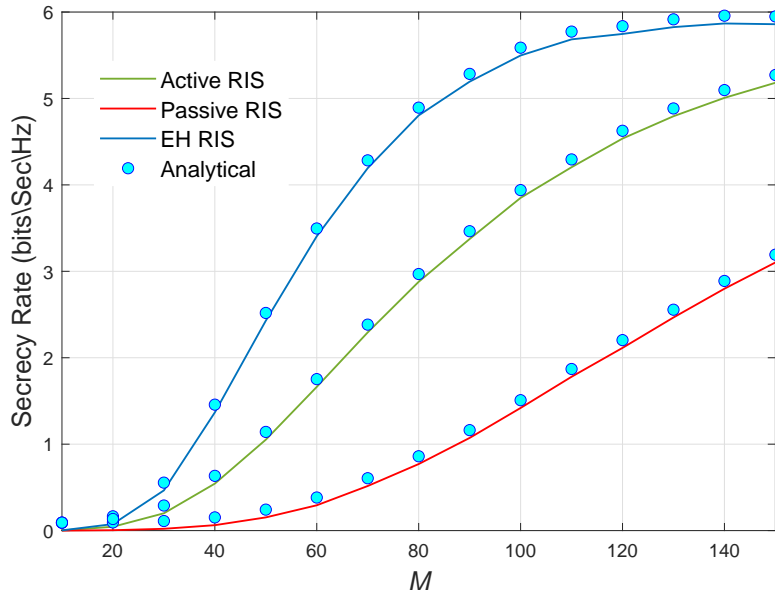


Figure 5: Secrecy rate versus number of RIS elements, M , with phase shift error.

number of the RIS elements, M , leads to an increase in the amount of the harvested energy at the RIS and thus P_r will be high when the number of elements M is very large.

In order to illustrate the RIS configuration selection scheme, in Fig. 6 we plot the user power versus the target secrecy rate for different values of the concentration parameter of RIS phase error, $\kappa = 2$ and 8. Firstly, in Figs. 6a and 6b, we consider two examples, when the target secrecy rate is assumed to be $r_s = 0.75$ (bits/s/Hz) and $r_s = 1.2$ (bits/s/Hz) for $\kappa = 2$ and 8. As we can see from

the results in Fig. 6a, when $r_s = 0.75$ (bits/s/Hz), passive RIS can achieve the target secrecy rate with total transmission power is $P_T = p_k = 50W$, (neglecting the small amount of power consuming at passive RIS elements), and in the active RIS scheme the user transmission power can be reduced to around $p_k = 7W$ and thus the total transmission power is $P_T = p_k + P_r = 14W$, while EH RIS scheme can achieve the target secrecy rate with the smallest amount of the user power which is about $p_k = 2.95W$, but with the highest total transmission power $P_T = p_k + P_b = 52.95W$. Similar observations can be noticed from the second scenario when $r_s = 1.2$ (bits/s/Hz), passive RIS achieves the target secrecy rate with the highest user power, while EH RIS achieves, r_s , with the smallest user power but with very high total consumption power, and the active RIS scheme works between these two regions. In addition, the concentration parameter of RIS phase error, κ , has essential impact on the required user power. By comparing Figs 6a and 6b, one can notice that as κ increases the required user power to achieve the target secrecy rate decreases. For instance when the target secrecy rate is $r_s = 0.75$ (bits/s/Hz), the required user power in the passive RIS scheme is about 50W when $\kappa = 2$, and 20W when $\kappa = 8$. This is due to the fact explained in Fig. 3.

Then, in Figs. 6c and 6d, we present the RIS configuration selection scheme when the available user power is $p_k = 20W$ for $\kappa = 2$ and 8. In the first case when $\kappa = 2$, if the target secrecy rate is $r_s \leq 0.45$ (bits/s/Hz), passive RIS can be selected, and active RIS can be implemented if the target secrecy rate is $r_s \leq 1.17$ (bits/s/Hz), while EH RIS can be selected if $r_s \leq 1.87$ (bits/s/Hz). These secrecy rate regions of the RIS schemes become wider as the concentration parameter of RIS phase error, κ , increases. In Fig. 6d when $\kappa = 8$, passive RIS can be selected to achieve secrecy rates up to $r_s \leq 0.77$ (bits/s/Hz), and active RIS can be selected to perform secrecy rates less than or equal to $r_s \leq 1.635$ (bits/s/Hz), whilst EH RIS can be used to achieve secrecy rates up to $r_s \leq 2.48$ (bits/s/Hz).

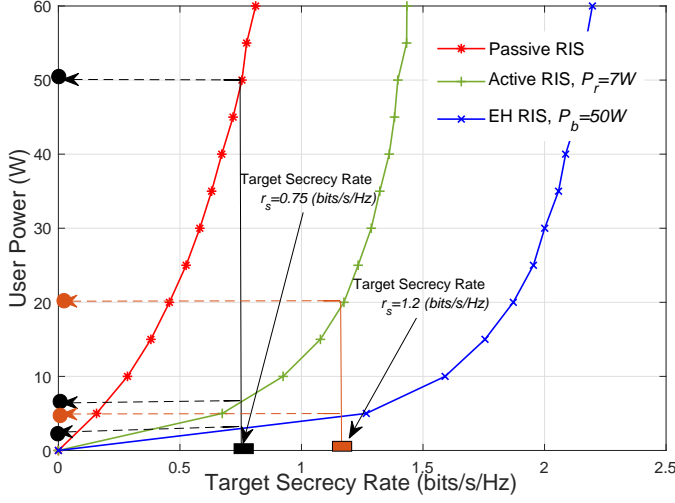
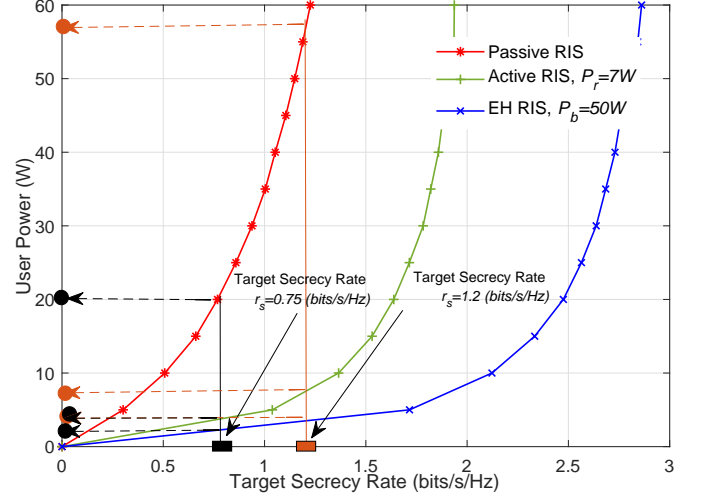
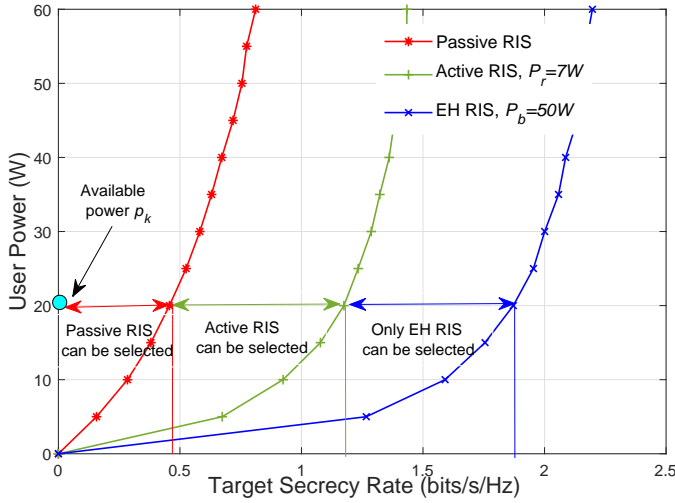
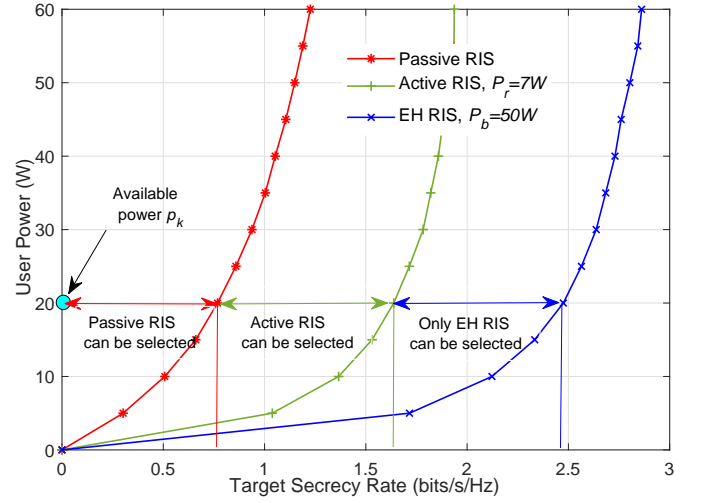
(a) The user power versus target secrecy rate when $\kappa = 2$.(b) The user power versus target secrecy rate when $\kappa = 8$.(c) RIS configuration selection scheme when $p_k = 20W$ and $\kappa = 2$.(d) RIS configuration selection scheme when $p_k = 20W$ and, $\kappa = 8$.

Figure 6: The user power versus target secrecy rate for different values of the concentration parameter of RIS phase error, κ .

VIII. CONCLUSIONS

In this paper the impact of phase shift error on the secrecy performance of up-link RIS-aided MU-MISO systems was considered. Under Rician fading channels and phase shift errors the ergodic secrecy rate for, passive RIS, active RIS, and EH RIS have been analyzed. Then, the phase shifts at the RIS have been optimized based on the derived rate expressions. In addition, according to the target secrecy rate and amount of power available at the users, the best RIS configuration selection scheme has been considered. The results presented in this work demonstrated that an active RIS scheme can enhance the secrecy performance of imperfect RIS elements, especially when the users have limited amount of

power. Furthermore, increasing the number of BS antennas, the concentration parameter of RIS phase error, and the number of RIS elements lead to the enhancement of the secrecy performance.

APPENDIX A

By using Jensen inequality, the ergodic rate can be expressed as

$$\mathcal{E} \{R_{b_k}\} \approx \log_2 \left(1 + \mathcal{E} \left\{ \frac{p_k L_{u_k,b} |\mathbf{h}_{r,k}^H \Theta^H \mathbf{G}^H \mathbf{G} \Theta \bar{\Theta} \mathbf{h}_{r,k}|^2}{\sum_{\substack{i=1 \\ i \neq k}}^K p_i L_{u_i,b} |\mathbf{h}_{r,k}^H \Theta^H \mathbf{G}^H \mathbf{G} \Theta \bar{\Theta} \mathbf{h}_{r,i}|^2 + \|\mathbf{h}_{r,k}^H \Theta^H \mathbf{G}^H\|^2 \sigma_b^2} \right\} \right). \quad (40)$$

Due to the paper length limitation, in this Appendix we will explain how to calculate the average of the first term, similarly and by following similar steps we can find the average of the other terms. The first term is

$$\mathcal{E} \left\{ P_k L_{u_k,b} |\mathbf{h}_{r,k}^H \Theta^H \mathbf{G}^H \mathbf{G} \Theta \bar{\Theta} \mathbf{h}_{r,k}|^2 \right\} = P_k L_{u_k,b} \mathcal{E} \left\{ |\mathbf{h}_{r,k}^H \Theta^H \mathbf{G}^H \mathbf{G} \Theta \bar{\Theta} \mathbf{h}_{r,k}|^2 \right\} \quad (41)$$

where

$$\begin{aligned} \mathbf{h}_{r,k}^H \Theta^H \mathbf{G}^H \mathbf{G} \Theta \bar{\Theta} \mathbf{h}_{r,k} &= \mathbf{h}_{r,k}^H \Theta^H \left(\frac{\rho_b}{\rho_b + 1} \bar{\mathbf{G}}^H \bar{\mathbf{G}} + \frac{\sqrt{\rho_b}}{\rho_b + 1} \bar{\mathbf{G}}^H \tilde{\mathbf{G}} + \frac{\sqrt{\rho_b}}{\rho_b + 1} \tilde{\mathbf{G}}^H \bar{\mathbf{G}} + \frac{1}{\rho_b + 1} \tilde{\mathbf{G}}^H \tilde{\mathbf{G}} \right) \Theta \bar{\Theta} \mathbf{h}_{r,k} \\ &= \frac{1}{\rho_b + 1} \mathbf{h}_{r,k}^H \Theta^H \left(\rho_b \bar{\mathbf{G}}^H \bar{\mathbf{G}} + \sqrt{\rho_b} \bar{\mathbf{G}}^H \tilde{\mathbf{G}} + \sqrt{\rho_b} \tilde{\mathbf{G}}^H \bar{\mathbf{G}} + \tilde{\mathbf{G}}^H \tilde{\mathbf{G}} \right) \Theta \bar{\Theta} \mathbf{h}_{r,k} = \frac{1}{\rho_b + 1} \mathbf{h}_{r,k}^H \mathbf{A} \bar{\Theta} \mathbf{h}_{r,k} \end{aligned} \quad (42)$$

where $\mathbf{A} = \Theta^H \left(\rho_b \bar{\mathbf{G}}^H \bar{\mathbf{G}} + \sqrt{\rho_b} \bar{\mathbf{G}}^H \tilde{\mathbf{G}} + \sqrt{\rho_b} \tilde{\mathbf{G}}^H \bar{\mathbf{G}} + \tilde{\mathbf{G}}^H \tilde{\mathbf{G}} \right) \Theta$. Now (42) can be expressed as

$$\begin{aligned} \mathbf{h}_{r,k}^H \Theta^H \mathbf{G}^H \mathbf{G} \Theta \bar{\Theta} \mathbf{h}_{r,k} &= \frac{1}{(\rho_b + 1)(\rho_k + 1)} \left(\sqrt{\rho_k} \bar{\mathbf{h}}_{r,k}^H + \tilde{\mathbf{h}}_{r,k}^H \right) \mathbf{A} \bar{\Theta} \left(\sqrt{\rho_k} \bar{\mathbf{h}}_{r,k} + \tilde{\mathbf{h}}_{r,k} \right) \\ &= \frac{1}{(\rho_b + 1)(\rho_k + 1)} \left(\underbrace{\rho_k \bar{\mathbf{h}}_{r,k}^H \mathbf{A} \bar{\Theta} \bar{\mathbf{h}}_{r,k}}_{\Delta_1} + \underbrace{\sqrt{\rho_k} \bar{\mathbf{h}}_{r,k}^H \mathbf{A} \bar{\Theta} \tilde{\mathbf{h}}_{r,k}}_{\Delta_2} + \underbrace{\sqrt{\rho_k} \tilde{\mathbf{h}}_{r,k}^H \mathbf{A} \bar{\Theta} \bar{\mathbf{h}}_{r,k}}_{\Delta_3} + \underbrace{\tilde{\mathbf{h}}_{r,k}^H \mathbf{A} \bar{\Theta} \tilde{\mathbf{h}}_{r,k}}_{\Delta_4} \right) \end{aligned} \quad (43)$$

The channels are independent and have zero mean. Thus by removing the zero expectation terms, we can get

$$\begin{aligned} \mathcal{E} \left\{ \left| \mathbf{h}_{r,k}^H \Theta^H \mathbf{G}^H \mathbf{G} \Theta \bar{\Theta} \mathbf{h}_{r,k} \right|^2 \right\} &= \frac{1}{(\rho_b + 1)^2 (\rho_k + 1)^2} \mathcal{E} \left\{ \left| \sum_{i=1}^4 \Delta_i \right|^2 \right\} \\ &= \frac{1}{(\rho_b + 1)^2 (\rho_k + 1)^2} \left(\sum_{i=1}^4 \mathcal{E} \{ |\Delta_i|^2 \} + 2 \mathcal{E} \{ \Delta_1 \Delta_4^* \} \right) \end{aligned} \quad (44)$$

Now the first term

$$\begin{aligned} \Delta_1 &= \rho_k \bar{\mathbf{h}}_{r,k}^H \Theta^H \left(\rho_b \bar{\mathbf{G}}^H \bar{\mathbf{G}} + \sqrt{\rho_b} \bar{\mathbf{G}}^H \tilde{\mathbf{G}} + \sqrt{\rho_b} \tilde{\mathbf{G}}^H \bar{\mathbf{G}} + \tilde{\mathbf{G}}^H \tilde{\mathbf{G}} \right) \Theta \bar{\Theta} \bar{\mathbf{h}}_{r,k} \\ &= \left(\underbrace{\rho_b \rho_k \bar{\mathbf{h}}_{r,k}^H \Theta^H \bar{\mathbf{G}}^H \bar{\mathbf{G}} \Theta \bar{\Theta} \bar{\mathbf{h}}_{r,k}}_{\Delta_{1,1}} + \underbrace{\sqrt{\rho_b} \rho_k \bar{\mathbf{h}}_{r,k}^H \Theta^H \bar{\mathbf{G}}^H \tilde{\mathbf{G}} \Theta \bar{\Theta} \bar{\mathbf{h}}_{r,k}}_{\Delta_{1,2}} \right. \\ &\quad \left. + \underbrace{\sqrt{\rho_b} \rho_k \bar{\mathbf{h}}_{r,k}^H \Theta^H \tilde{\mathbf{G}}^H \bar{\mathbf{G}} \Theta \bar{\Theta} \bar{\mathbf{h}}_{r,k}}_{\Delta_{1,3}} + \underbrace{\rho_k \bar{\mathbf{h}}_{r,k}^H \Theta^H \tilde{\mathbf{G}}^H \tilde{\mathbf{G}} \Theta \bar{\Theta} \bar{\mathbf{h}}_{r,k}}_{\Delta_{1,4}} \right) \end{aligned} \quad (45)$$

The average of the first term

$$\mathcal{E} \{ |\Delta_1|^2 \} = \mathcal{E} \{ |\Delta_{1,1}|^2 \} + \mathcal{E} \{ |\Delta_{1,2}|^2 \} + \mathcal{E} \{ |\Delta_{1,3}|^2 \} + \mathcal{E} \{ |\Delta_{1,4}|^2 \} + 2 \mathcal{E} \{ \Delta_{1,1} \Delta_{1,4}^H \} \quad (46)$$

where $\Delta_{1,1} = \rho_b \rho_k \bar{\mathbf{h}}_{r,k}^H \Theta^H \bar{\mathbf{G}}^H \bar{\mathbf{G}} \Theta \bar{\Theta} \bar{\mathbf{h}}_{r,k}$, which can be written as

$$\Delta_{1,1} = \rho_b \rho_k \mathbf{a}_M^H(\phi_{kr}^a, \phi_{kr}^e) \Theta^H \mathbf{a}_M^H(\phi_r^a, \phi_r^e) \mathbf{a}_M(\phi_r^a, \phi_r^e) \Theta \bar{\Theta} \mathbf{a}_M(\phi_{kr}^a, \phi_{kr}^e),$$

$$\Delta_{1,1} = \rho_b \rho_k \left(\sum_{m=1}^M a_{M,m}^H(\phi_{kr}^a, \phi_{kr}^e) e^{-j\varphi_m} a_{M,m}^H(\phi_r^a, \phi_r^e) \right) \left(\sum_{m=1}^M a_{M,m}(\phi_{kr}^a, \phi_{kr}^e) e^{j\varphi_m} e^{j\varphi_m} a_{M,m}(\phi_r^a, \phi_r^e) \right). \quad (47)$$

The average can now be written as

$$\begin{aligned}
\mathcal{E} \{ |\Delta_{1,1}|^2 \} &= \rho_b^2 \rho_k^2 \left(\sum_{m=1}^M a_{M,m}^H(\phi_{kr}^a, \phi_{kr}^e) e^{-j\varphi_m} a_{M,m}^H(\phi_r^a, \phi_r^e) \right)^2 \\
&\times \left(M + \rho(\kappa)^2 \left| \sum_{m_1=1}^M \sum_{m_2 \neq m_1}^M (a_{M,m_1}(\phi_{kr}^a, \phi_{kr}^e) e^{j\varphi_{m_1}} a_{M,m_1}(\phi_r^a, \phi_r^e)) (a_{M,m_2}(\phi_{kr}^a, \phi_{kr}^e) e^{j\varphi_{m_2}} a_{M,m_2}(\phi_r^a, \phi_r^e))^H \right|^2 \right)
\end{aligned} \tag{48}$$

$$\mathcal{E} \{ |\Delta_{1,1}|^2 \} = \rho_b^2 \rho_k^2 |f_k|^2 ((1 - \rho(\kappa)^2) M + \rho(\kappa)^2 |f_k|^2) \tag{49}$$

where $f_k = \sum_{m=1}^M f_{k,m}$, $f_{k,m} = a_{M,m}^H(\phi_r^a, \phi_r^e) e^{j\varphi_m} a_{M,m}(\phi_{kr}^a, \phi_{kr}^e)$. The second term,

$$\begin{aligned}
\Delta_{1,2} &= \sqrt{\rho_b} \rho_k a_M^H(\phi_{kr}^a, \phi_{kr}^e) \Theta^H a_M(\phi_r^a, \phi_r^e) a_N^H(\phi_b^a, \phi_b^e) \tilde{\mathbf{G}} \Theta \bar{\Theta} a_M(\phi_{kr}^a, \phi_{kr}^e) \\
&= \sqrt{\rho_b} \rho_k f_k^* \sum_{m=1}^M \sum_{n=1}^N a_{N,n}^H(\phi_b^a, \phi_b^e) \tilde{\mathbf{g}}_{nm} e^{j\varphi_m} e^{j\bar{\varphi}_m} a_{M,m}(\phi_{kr}^a, \phi_{kr}^e),
\end{aligned} \tag{50}$$

$$\mathcal{E} \{ |\Delta_{1,2}|^2 \} = \rho_b \rho_k^2 N M |f_k|^2. \tag{51}$$

The third term

$$\begin{aligned}
\Delta_{1,3} &= \sqrt{\rho_b} \rho_k a_M^H(\phi_{kr}^a, \phi_{kr}^e) \Theta^H \tilde{\mathbf{G}}^H a_N(\phi_b^a, \phi_b^e) a_M^H(\phi_r^a, \phi_r^e) \Theta \bar{\Theta} a_M(\phi_{kr}^a, \phi_{kr}^e) \\
&= \sqrt{\rho_b} \rho_k \sum_{m=1}^M \sum_{n=1}^N a_{N,n}^H(\phi_b^a, \phi_b^e) \tilde{g}_{nm}^H e^{-j\varphi_m} a_{M,m}(\phi_{kr}^a, \phi_{kr}^e) \sum_{m=1}^M e^{j\bar{\varphi}_m} f_{k,m},
\end{aligned} \tag{52}$$

$$\mathcal{E} \{ |\Delta_{1,3}|^2 \} = \rho_b \rho_k^2 (N M \rho(\kappa)^2 |f_k|^2 + (1 - \rho(\kappa)^2) N M^2). \tag{53}$$

The forth term

$$\Delta_{1,4} = \rho_k a_M^H(\phi_{kr}^a, \phi_{kr}^e) \Theta^H \tilde{\mathbf{G}}^H \tilde{\mathbf{G}} \Theta \bar{\Theta} a_M(\phi_{kr}^a, \phi_{kr}^e)$$

$$= \rho_k \sum_{m_1=1}^M a_{M,m_1}^H (\phi_{kr}^a, \phi_{kr}^e) e^{-j\varphi_m} \tilde{g}_{nm_1}^H \sum_{m_2=1}^M \tilde{g}_{nm_2} e^{j\varphi_m} e^{j\varphi_m} a_{M,m_2} (\phi_{kr}^a, \phi_{kr}^e), \quad (54)$$

$$\mathcal{E} \{ |\Delta_{1,4}|^2 \} = \rho_k NM (M\rho(\kappa)^2 + 1 - \rho(\kappa)^2) + NM^2. \quad (55)$$

The last term

$$\mathcal{E} \{ \Delta_{1,1} \Delta_{1,4}^* \} = N |f_k|^2 (M\rho(\kappa)^2 + 1 - \rho(\kappa)^2). \quad (56)$$

Similarly, following the same way we can find the average of the other terms.

APPENDIX B

Using Jensen inequality, the ergodic rate can be written as

$$\mathcal{E} \{ R_{e_j,k} \} \approx \log_2 \left(1 + \mathcal{E} \left\{ \frac{p_k \left| d_{u_k,r}^{-\frac{\alpha_r}{2}} d_{e_j,r}^{-\frac{\alpha_e}{2}} \mathbf{h}_{e_j,r} \Theta \bar{\Theta} \mathbf{h}_{r,k} + d_{e_j,k}^{-\frac{\alpha_e}{2}} h_{e_j,k} \right|^2}{\sum_{\substack{i=1 \\ i \neq k}}^K p_i \left| d_{u_i,r}^{-\frac{\alpha_r}{2}} d_{e_j,r}^{-\frac{\alpha_e}{2}} \mathbf{h}_{e_j,r} \Theta \bar{\Theta} \mathbf{h}_{r,i} + d_{e_j,i}^{-\frac{\alpha_e}{2}} h_{e_j,i} \right|^2 + \sigma_{e_j}^2} \right\} \right) \quad (57)$$

The average of the first term, after removing the zero expectation terms can be calculated by,

$$\mathcal{E} \left\{ \left| d_{u_k,r}^{-\frac{\alpha_r}{2}} d_{e_j,r}^{-\frac{\alpha_e}{2}} \mathbf{h}_{e_j,r} \Theta \bar{\Theta} \mathbf{h}_{r,k} + d_{e_j,k}^{-\frac{\alpha_e}{2}} h_{e_j,k} \right|^2 \right\} = d_{u_k,r}^{-\alpha_r} d_{e_j,r}^{-\alpha_e} \mathcal{E} \left\{ \left| \mathbf{h}_{e_j,r} \Theta \bar{\Theta} \mathbf{h}_{r,k} \right|^2 \right\} + d_{e_j,r}^{-\alpha_e} \quad (58)$$

where

$$\begin{aligned} \mathcal{E} \left\{ \left| \mathbf{h}_{e_j,r} \Theta \bar{\Theta} \mathbf{h}_{r,k} \right|^2 \right\} &= \mathcal{E} \left\{ \left| \left(\sqrt{\frac{\rho_{e_j}}{\rho_{e_j} + 1}} \sqrt{\frac{\rho_k}{\rho_k + 1}} \bar{\mathbf{h}}_{e_j} \Theta \bar{\Theta} \bar{\mathbf{h}}_{r,k} + \sqrt{\frac{\rho_{e_j}}{\rho_{e_j} + 1}} \sqrt{\frac{1}{\rho_k + 1}} \bar{\mathbf{h}}_{e_j} \Theta \bar{\Theta} \tilde{\mathbf{h}}_{r,k} \right. \right. \right. \\ &\quad \left. \left. \left. + \sqrt{\frac{\rho_k}{\rho_k + 1}} \sqrt{\frac{1}{\rho_{e_j} + 1}} \tilde{\mathbf{h}}_{e_j} \Theta \bar{\Theta} \bar{\mathbf{h}}_{r,k} + \sqrt{\frac{1}{\rho_{e_j} + 1}} \sqrt{\frac{1}{\rho_k + 1}} \tilde{\mathbf{h}}_{e_j} \Theta \bar{\Theta} \tilde{\mathbf{h}}_{r,k} \right) \right|^2 \right\} \quad (59) \end{aligned}$$

$$\mathcal{E} \left\{ \left| \mathbf{h}_{e_j,r} \Theta \bar{\Theta} \mathbf{h}_{r,k} \right|^2 \right\} = \frac{\rho_{e_j}}{\rho_{e_j} + 1} \frac{\rho_k}{\rho_k + 1} \mathcal{E} \left\{ \left| \bar{\mathbf{h}}_{e_j} \Theta \bar{\Theta} \bar{\mathbf{h}}_{r,k} \right|^2 \right\} + \frac{\rho_{e_j}}{\rho_{e_j} + 1} \frac{1}{\rho_k + 1} \mathcal{E} \left\{ \left| \bar{\mathbf{h}}_{e_j} \Theta \bar{\Theta} \tilde{\mathbf{h}}_{r,k} \right|^2 \right\}$$

$$+ \frac{\rho_k}{\rho_k + 1} \frac{1}{\rho_{e_j} + 1} \mathcal{E} \left| \tilde{\mathbf{h}}_{e_j} \Theta \bar{\Theta} \tilde{\mathbf{h}}_{r,k} \right|^2 + \frac{1}{\rho_{e_j} + 1} \frac{1}{\rho_k + 1} \mathcal{E} \left| \tilde{\mathbf{h}}_{e_j} \Theta \bar{\Theta} \tilde{\mathbf{h}}_{r,k} \right|^2 \quad (60)$$

Now

$$\bar{\mathbf{h}}_{e_j} \Theta \bar{\Theta} \tilde{\mathbf{h}}_{r,k} = \left(\sum_{m=1}^M a_{M,m} (\phi_{kr}^a, \phi_{kr}^e) e^{j\varphi_m} e^{j\bar{\varphi}_m} a_{M,m} (\phi_{e_j r}^a, \phi_{e_j r}^e) \right) \quad (61)$$

$$\mathcal{E} \left| \bar{\mathbf{h}}_{e_j} \Theta \bar{\Theta} \tilde{\mathbf{h}}_{r,k} \right|^2 = \mathcal{E} \left| \sum_{m=1}^M a_{M,m} (\phi_{kr}^a, \phi_{kr}^e) e^{j\varphi_m} e^{j\bar{\varphi}_m} a_{M,m} (\phi_{e_j r}^a, \phi_{e_j r}^e) \right|^2$$

$$= M + \rho(\kappa)^2 \sum_{m_1=1}^M \sum_{m_2 \neq m_1}^M (a_{M,m_1} (\phi_{kr}^a, \phi_{kr}^e) e^{j\varphi_{m_1}} a_{M,m_1} (\phi_r^a, \phi_r^e)) (a_{M,m_2} (\phi_{kr}^a, \phi_{kr}^e) e^{j\varphi_{m_2}} a_{M,m_2} (\phi_r^a, \phi_r^e))^H \\ = M + \rho(\kappa)^2 \xi \quad (62)$$

$$\text{where } \xi = \sum_{m_1=1}^M \sum_{m_2 \neq m_1}^M (a_{M,m_1} (\phi_{kr}^a, \phi_{kr}^e) e^{j\varphi_{m_1}} a_{M,m_1} (\phi_r^a, \phi_r^e)) (a_{M,m_2} (\phi_{kr}^a, \phi_{kr}^e) e^{j\varphi_{m_2}} a_{M,m_2} (\phi_r^a, \phi_r^e))^H.$$

Similarly, the second term,

$$\bar{\mathbf{h}}_{e_j} \Theta \bar{\Theta} \tilde{\mathbf{h}}_{r,k} = \mathbf{a}_M (\phi_{e_j r}^a, \phi_{e_j r}^e) \Theta \bar{\Theta} \tilde{\mathbf{h}}_{r,k} = \sum_{m=1}^M a_{Mm} (\phi_{e_j r}^a, \phi_{e_j r}^e) e^{j\varphi_m} e^{j\bar{\varphi}_m} [\tilde{h}_{r,k}]_m \quad (63)$$

$$\mathcal{E} \left| \bar{\mathbf{h}}_{e_j} \Theta \bar{\Theta} \tilde{\mathbf{h}}_{r,k} \right|^2 = \mathcal{E} \left| \sum_{m=1}^M a_{Mm} (\phi_{e_j r}^a, \phi_{e_j r}^e) e^{j\varphi_m} e^{j\bar{\varphi}_m} [\tilde{h}_{r,k}]_m \right|^2$$

$$\mathcal{E} \left| \bar{\mathbf{h}}_{e_j} \Theta \bar{\Theta} \tilde{\mathbf{h}}_{r,k} \right|^2 = M +$$

$$\mathcal{E} \left\{ \sum_{m_1=1}^M \sum_{m_2 \neq m_1}^M \left(a_{Mm_1} (\phi_{e_j r}^a, \phi_{e_j r}^e) e^{j\varphi_{m_1}} e^{j\bar{\varphi}_{m_1}} [\tilde{h}_{r,k}]_{m_1} \right) \left(a_{Mm_2} (\phi_{e_j r}^a, \phi_{e_j r}^e) e^{j\varphi_{m_2}} e^{j\bar{\varphi}_{m_2}} [\tilde{h}_{r,k}]_{m_2} \right)^H \right\} = M \quad (64)$$

other terms,

$$\tilde{\mathbf{h}}_{e_j} \Theta \bar{\Theta} \bar{\mathbf{h}}_{r,k} = \sum_{m=1}^M \tilde{h}_{e_j,m} e^{j\varphi_m} e^{j\bar{\varphi}_m} a_{M,m}(\phi_{kr}^a, \phi_{kr}^e) \quad (65)$$

$$\mathcal{E} \left| \tilde{\mathbf{h}}_{e_j} \Theta \bar{\Theta} \bar{\mathbf{h}}_{r,k} \right|^2 = M +$$

$$\mathcal{E} \left\{ \sum_{m_1=1}^M \sum_{m_2 \neq m_1}^M \left(\left[\tilde{h}_{e_j} \right]_{m_1} e^{j\varphi_{m_1}} e^{j\bar{\varphi}_{m_1}} a_{M,m_1}(\phi_{kr}^a, \phi_{kr}^e) \right) \left(\left[\tilde{h}_{e_j} \right]_{m_2} e^{j\varphi_{m_2}} e^{j\bar{\varphi}_{m_2}} a_{M,m_2}(\phi_{kr}^a, \phi_{kr}^e) \right)^H \right\} = M \quad (66)$$

and

$$\tilde{\mathbf{h}}_{e_j} \Theta \bar{\Theta} \tilde{\mathbf{h}}_{r,k} = \sum_{m=1}^M \left[\tilde{h}_{e_j} \right]_m e^{j\varphi_m} e^{j\bar{\varphi}_m} \left[\tilde{h}_{r,k} \right]_m \quad (67)$$

$$\mathcal{E} \left| \tilde{\mathbf{h}}_{e_j} \Theta \bar{\Theta} \tilde{\mathbf{h}}_{r,k} \right|^2 = \mathcal{E} \left| \sum_{m=1}^M \left[\tilde{h}_{e_j} \right]_m e^{j\varphi_m} e^{j\bar{\varphi}_m} \left[\tilde{h}_{r,k} \right]_m \right|^2 = M \quad (68)$$

Now, we are ready to write the average of the first term,

$$\begin{aligned} \mathcal{E} \left\{ \left| \mathbf{h}_{e_j,r} \Theta \bar{\Theta} \mathbf{h}_{r,k} \right|^2 \right\} &= \frac{\rho_{e_j}}{\rho_{e_j} + 1} \frac{\rho_k}{\rho_k + 1} (M + \rho(\kappa)^2 \xi) + \frac{\rho_{e_j}}{\rho_{e_j} + 1} \frac{1}{\rho_k + 1} M \\ &+ \frac{\rho_k}{\rho_k + 1} \frac{1}{\rho_{e_j} + 1} M + \frac{1}{\rho_{e_j} + 1} \frac{1}{\rho_k + 1} M \end{aligned} \quad (69)$$

Similarly we can find the average of the second term as,

$$\mathcal{E} \left\{ \left| d_{u_i,r}^{-\frac{\alpha_r}{2}} d_{e_j,r}^{-\frac{\alpha_e}{2}} \mathbf{h}_{e_j,r} \Theta \bar{\Theta} \mathbf{h}_{r,i} + d_{e_j,i}^{-\frac{\alpha_e}{2}} h_{e_j,i} \right|^2 \right\} = d_{u_i,r}^{-\alpha_r} d_{e_j,r}^{-\alpha_e} \mathcal{E} \left\{ \left| \mathbf{h}_{e_j,r} \Theta \bar{\Theta} \mathbf{h}_{r,i} \right|^2 \right\} + d_{e_j,i}^{-\alpha_e} \quad (70)$$

$$\begin{aligned} \mathcal{E} \left\{ \left| \mathbf{h}_{e_j,r} \Theta \bar{\Theta} \mathbf{h}_{r,i} \right|^2 \right\} &= \frac{\rho_{e_j}}{\rho_{e_j} + 1} \frac{\rho_i}{\rho_i + 1} (M + \rho(\kappa)^2 \xi) + \frac{\rho_{e_j}}{\rho_{e_j} + 1} \frac{1}{\rho_i + 1} M \\ &+ \frac{\rho_i}{\rho_i + 1} \frac{1}{\rho_{e_j} + 1} M + \frac{1}{\rho_{e_j} + 1} \frac{1}{\rho_i + 1} M \end{aligned} \quad (71)$$

APPENDIX C

Using Jensen inequality, the ergodic rate can be written as

$$\mathcal{E} \{R_{b_k}\} \approx \log_2 (1 + \mathcal{E} \{\gamma_{b_k}\}) \quad (72)$$

We will follow similar steps as in Appendix A,

$$\mathbf{h}_{r,k}^H \Theta^H \mathbf{G}^H \mathbf{G} \bar{\Theta} \Theta = \frac{1}{\rho_b + 1} \mathbf{h}_{r,k}^H \mathbf{A} \bar{\Theta} \quad (73)$$

where $\mathbf{A} = \Theta^H \left(\rho_b \bar{\mathbf{G}}^H \bar{\mathbf{G}} + \sqrt{\rho_b} \bar{\mathbf{G}}^H \tilde{\mathbf{G}} + \sqrt{\rho_b} \tilde{\mathbf{G}}^H \bar{\mathbf{G}} + \tilde{\mathbf{G}}^H \tilde{\mathbf{G}} \right) \Theta$. Last expression can be written as

$$\begin{aligned} \mathbf{h}_{r,k}^H \Theta^H \mathbf{G}^H \mathbf{G} \bar{\Theta} \Theta &= \frac{1}{(\rho_b + 1) \sqrt{(\rho_k + 1)}} \left(\sqrt{\rho_k} \bar{\mathbf{h}}_{r,k}^H + \tilde{\mathbf{h}}_{r,k}^H \right) \mathbf{A} \bar{\Theta} \\ &= \frac{1}{(\rho_b + 1) \sqrt{(\rho_k + 1)}} \left(\underbrace{\sqrt{\rho_k} \bar{\mathbf{h}}_{r,k}^H \mathbf{A} \bar{\Theta}}_{\Delta_1} + \underbrace{\tilde{\mathbf{h}}_{r,k}^H \mathbf{A} \bar{\Theta}}_{\Delta_2} \right) \end{aligned} \quad (74)$$

The average can be written as,

$$\mathcal{E} \left\{ \left\| \mathbf{h}_{r,k}^H \Theta^H \mathbf{G}^H \mathbf{G} \bar{\Theta} \Theta \right\|^2 \right\} = \frac{1}{(\rho_b + 1)^2 (\rho_k + 1)} \mathcal{E} \left\{ \rho_r \left\| \underbrace{\bar{\mathbf{h}}_{r,k}^H \mathbf{A} \bar{\Theta}}_{\Delta_1} \right\|^2 + \left\| \underbrace{\tilde{\mathbf{h}}_{r,k}^H \mathbf{A} \bar{\Theta}}_{\Delta_2} \right\|^2 \right\} \quad (75)$$

$$\begin{aligned} \Delta_1 &= \sqrt{\rho_k} \bar{\mathbf{h}}_{r,k}^H \Theta^H \left(\rho_b \bar{\mathbf{G}}^H \bar{\mathbf{G}} + \sqrt{\rho_b} \bar{\mathbf{G}}^H \tilde{\mathbf{G}} + \sqrt{\rho_b} \tilde{\mathbf{G}}^H \bar{\mathbf{G}} + \tilde{\mathbf{G}}^H \tilde{\mathbf{G}} \right) \Theta \bar{\Theta} \\ &= \left(\underbrace{\rho_b \sqrt{\rho_k} \bar{\mathbf{h}}_{r,k}^H \Theta^H \bar{\mathbf{G}}^H \bar{\mathbf{G}} \Theta \bar{\Theta}}_{\Delta_{1,1}} + \underbrace{\sqrt{\rho_b} \sqrt{\rho_k} \bar{\mathbf{h}}_{r,k}^H \Theta^H \bar{\mathbf{G}}^H \tilde{\mathbf{G}} \Theta \bar{\Theta}}_{\Delta_{1,2}} \right. \\ &\quad \left. + \underbrace{\sqrt{\rho_b} \sqrt{\rho_k} \bar{\mathbf{h}}_{r,k}^H \Theta^H \tilde{\mathbf{G}}^H \bar{\mathbf{G}} \Theta \bar{\Theta}}_{\Delta_{1,3}} + \underbrace{\sqrt{\rho_k} \bar{\mathbf{h}}_{r,k}^H \Theta^H \tilde{\mathbf{G}}^H \tilde{\mathbf{G}} \Theta \bar{\Theta}}_{\Delta_{1,4}} \right) \end{aligned} \quad (76)$$

$$\mathcal{E} \{|\Delta_1|^2\} = \mathcal{E} \{|\Delta_{1,1}|^2\} + \mathcal{E} \{|\Delta_{1,2}|^2\} + \mathcal{E} \{|\Delta_{1,3}|^2\} + \mathcal{E} \{|\Delta_{1,4}|^2\} + 2\mathcal{E} \{\Delta_{1,1} \Delta_{1,4}^H\} \quad (77)$$

where

$$\Delta_{1,1} = \rho_b \sqrt{\rho_k} \left(a_M^H(\phi_{kr}^a, \phi_{kr}^e) \Theta^H a_M^H(\phi_r^a, \phi_r^e) a_N^H(\phi_b^a, \phi_b^e) a_N(\phi_b^a, \phi_b^e) \right) \left(a_M(\phi_r^a, \phi_r^e) \Theta \bar{\Theta} \right) \quad (78)$$

$$\begin{aligned} \mathcal{E} \{ |\Delta_{1,1}|^2 \} &= \rho_b^2 \rho_k \left| \left(a_M^H(\phi_{kr}^a, \phi_{kr}^e) \Theta^H a_M^H(\phi_r^a, \phi_r^e) a_N^H(\phi_b^a, \phi_b^e) a_N(\phi_b^a, \phi_b^e) \right) \right|^2 \\ &\times \mathcal{E} \left\{ \left\| a_M(\phi_r^a, \phi_r^e) \Theta \bar{\Theta} \right\|^2 \right\} \end{aligned} \quad (79)$$

$$\mathcal{E} \{ |\Delta_{1,1}|^2 \} = \rho_b^2 \rho_k \left| \left(a_M^H(\phi_{kr}^a, \phi_{kr}^e) \Theta^H a_M^H(\phi_r^a, \phi_r^e) a_N^H(\phi_b^a, \phi_b^e) a_N(\phi_b^a, \phi_b^e) \right) \right|^2 \times M \quad (80)$$

The second term can be expressed as,

$$\Delta_{1,2} = \sqrt{\rho_b} \sqrt{\rho_k} a_M^H(\phi_{kr}^a, \phi_{kr}^e) \Theta^H a_M(\phi_r^a, \phi_r^e) \sum_{m=1}^M \sum_{n=1}^N a_{N,n}^H(\phi_b^a, \phi_b^e) \tilde{\mathbf{g}}_{nm} e^{j\varphi_m} e^{j\bar{\varphi}_m} \quad (81)$$

$$\mathcal{E} \{ |\Delta_{1,2}|^2 \} = \rho_b \rho_k \left| a_M^H(\phi_{kr}^a, \phi_{kr}^e) \Theta^H a_M(\phi_r^a, \phi_r^e) \right|^2 N M \quad (82)$$

The third term can be written as

$$\Delta_{1,3} = \sqrt{\rho_b} \sqrt{\rho_k} \sum_{m=1}^M \sum_{n=1}^N a_{M,m}^H(\phi_{kr}^a, \phi_{kr}^e) \tilde{g}_{nm}^H e^{-j\varphi_m} a_{N,n}(\phi_b^a, \phi_b^e) \sum_{m=1}^M a_{M,m}^H(\phi_r^a, \phi_r^e) e^{j\bar{\varphi}_m} e^{j\varphi_m} \quad (83)$$

$$\mathcal{E} \{ |\Delta_{1,3}|^2 \} = \rho_b \rho_k M N \left(\mathcal{E} \left| \sum_{m=1}^M a_{M,m}^H(\phi_r^a, \phi_r^e) e^{j\bar{\varphi}_m} e^{j\varphi_m} \right|^2 \right) \quad (84)$$

$$\mathcal{E} \{ |\Delta_{1,3}|^2 \} = \rho_b \rho_k M N \left(M + \rho(\kappa)^2 \sum_{m_1=1}^M \sum_{m_2 \neq m_1}^M a_{M,m_1}^H(\phi_r^a, \phi_r^e) e^{j\varphi_{m_1}} a_{M,m_2}(\phi_r^a, \phi_r^e) e^{-j\varphi_{m_2}} \right) \quad (85)$$

$$\mathcal{E} \{ |\Delta_{1,3}|^2 \} = \rho_b \rho_k M N \left(\rho(\kappa)^2 M + (1 - \rho(\kappa)^2) M \right) \quad (86)$$

The forth term can be represented as,

$$\Delta_{1,4} = \sqrt{\rho_k} \sum_{n=1}^N \sum_{m_1=1}^M a_{M,m_1}^H (\phi_{kr}^a, \phi_{kr}^e) e^{-j\varphi_m} \tilde{g}_{nm_1}^H \sum_{m_2=1}^M \tilde{g}_{nm_2} e^{j\varphi_m} e^{j\varphi_m} \quad (87)$$

$$\mathcal{E} \{ |\Delta_{1,4}|^2 \} = \rho_k (N^2 M + NM^2) \quad (88)$$

Now the last term can be written as

$$\begin{aligned} \mathcal{E} \{ \Delta_{1,1} \Delta_{1,4}^* \} &= \rho_b \rho_k (a_M^H (\phi_{kr}^a, \phi_{kr}^e) \Theta^H a_M^H (\phi_r^a, \phi_r^e) a_N^H (\phi_b^a, \phi_b^e) a_N (\phi_b^a, \phi_b^e)) \\ &\quad \times (a_M (\phi_r^a, \phi_r^e) \Theta \bar{\Theta}) \rho_k \tilde{\mathbf{h}}_{r,k}^H \Theta^H \tilde{\mathbf{G}}^H \tilde{\mathbf{G}} \Theta \bar{\Theta} \end{aligned} \quad (89)$$

$$\mathcal{E} \{ \Delta_{1,1} \Delta_{1,4}^* \} = \rho_b \rho_k (a_M^H (\phi_{kr}^a, \phi_{kr}^e) \Theta^H a_M^H (\phi_r^a, \phi_r^e) a_N^H (\phi_b^a, \phi_b^e) a_N (\phi_b^a, \phi_b^e)) (a_M (\phi_r^a, \phi_r^e) \Theta) \rho_k \tilde{\mathbf{h}}_{r,k}^H \Theta^H N \Theta \quad (90)$$

We will repeat similar steps for Δ_2 ,

$$\begin{aligned} \Delta_2 &= \left(\underbrace{\rho_b \tilde{\mathbf{h}}_{r,k}^H \Theta^H \tilde{\mathbf{G}}^H \tilde{\mathbf{G}} \Theta \bar{\Theta}}_{\Delta_{2,1}} + \underbrace{\sqrt{\rho_b} \tilde{\mathbf{h}}_{r,k}^H \Theta^H \tilde{\mathbf{G}}^H \tilde{\mathbf{G}} \Theta \bar{\Theta}}_{\Delta_{2,2}} \right. \\ &\quad \left. + \underbrace{\sqrt{\rho_b} \tilde{\mathbf{h}}_{r,k}^H \Theta^H \tilde{\mathbf{G}}^H \tilde{\mathbf{G}} \Theta \bar{\Theta}}_{\Delta_{2,3}} + \underbrace{\tilde{\mathbf{h}}_{r,k}^H \Theta^H \tilde{\mathbf{G}}^H \tilde{\mathbf{G}} \Theta \bar{\Theta}}_{\Delta_{2,4}} \right) \end{aligned} \quad (91)$$

$$\mathcal{E} \{ |\Delta_2|^2 \} = \mathcal{E} \{ |\Delta_{2,1}|^2 \} + \mathcal{E} \{ |\Delta_{2,2}|^2 \} + \mathcal{E} \{ |\Delta_{2,3}|^2 \} + \mathcal{E} \{ |\Delta_{2,4}|^2 \} + 2\mathcal{E} \{ \Delta_{2,1} \Delta_{2,4}^H \} \quad (92)$$

where

$$\Delta_{2,1} = \rho_b \tilde{\mathbf{h}}_{r,k}^H \Theta^H \tilde{\mathbf{G}}^H \tilde{\mathbf{G}} \Theta \bar{\Theta} \quad (93)$$

$$\mathcal{E} \{ |\Delta_{2,1}|^2 \} = \rho_b^2 \left\| \Theta^H a_M^H(\phi_r^a, \phi_r^e) a_N^H(\phi_b^a, \phi_b^e) a_N(\phi_b^a, \phi_b^e) a_M(\phi_r^a, \phi_r^e) \Theta \right\|_F^2 \quad (94)$$

and

$$\Delta_{2,2} = \sqrt{\rho_b} \tilde{\mathbf{h}}_{r,k}^H \Theta^H a_M(\phi_r^a, \phi_r^e) \sum_{m=1}^M \sum_{n=1}^N a_{N,n}^H(\phi_b^a, \phi_b^e) \tilde{\mathbf{g}}_{nm} e^{j\varphi_m} e^{j\bar{\varphi}_m} \quad (95)$$

$$\mathcal{E} \{ |\Delta_{2,2}|^2 \} = \rho_b \left| \tilde{\mathbf{h}}_{r,k}^H \Theta^H a_M(\phi_r^a, \phi_r^e) \right|^2 N M \quad (96)$$

while

$$\Delta_{2,3} = \sqrt{\rho_b} \sum_{m=1}^M \sum_{n=1}^N \tilde{h}_{r,k,nm}^H \tilde{g}_{nm}^H e^{-j\varphi_m} a_{N,n}(\phi_b^a, \phi_b^e) \sum_{m=1}^M a_{M,m}^H(\phi_r^a, \phi_r^e) e^{j\bar{\varphi}_m} e^{j\varphi_m} \quad (97)$$

$$\mathcal{E} \{ |\Delta_{2,3}|^2 \} = \rho_b M N \left(\mathcal{E} \left| \sum_{m=1}^M a_{M,m}^H(\phi_r^a, \phi_r^e) e^{j\bar{\varphi}_m} e^{j\varphi_m} \right|^2 \right) = \rho_b M N (\rho(\kappa)^2 M + (1 - \rho(\kappa)^2) M) \quad (98)$$

Finally,

$$\Delta_{2,4} = \rho_k \sum_{n=1}^N \sum_{m_1=1}^M \tilde{h}_{r,k,nm_1}^H e^{-j\varphi_{m_1}} \tilde{g}_{nm_1}^H \sum_{m_2=1}^M \tilde{g}_{nm_2} e^{j\varphi_{m_2}} e^{j\bar{\varphi}_{m_2}} \quad (99)$$

$$\mathcal{E} \{ |\Delta_{2,4}|^2 \} = \rho_k^2 (N^2 M + N M^2) \quad (100)$$

and

$$\mathcal{E} \{ \Delta_{2,1} \Delta_{2,4}^* \} = \mathcal{E} \left\{ \rho_b \rho_k \left(\tilde{\mathbf{h}}_{r,k}^H \Theta^H a_M^H(\phi_r^a, \phi_r^e) a_N^H(\phi_b^a, \phi_b^e) a_N(\phi_b^a, \phi_b^e) \right) (a_M(\phi_r^a, \phi_r^e) \Theta \bar{\Theta}) \rho_k \tilde{\mathbf{h}}_{r,k}^H \Theta^H \tilde{\mathbf{G}}^H \tilde{\mathbf{G}} \Theta \bar{\Theta} \right\}$$

$$= \rho_k \left(\Theta^H a_M^H(\phi_r^a, \phi_r^e) a_N^H(\phi_b^a, \phi_b^e) a_N(\phi_b^a, \phi_b^e) \right) (a_M(\phi_r^a, \phi_r^e) \Theta) \rho_k \Theta N \Theta^H \quad (101)$$

REFERENCES

- [1] M. Di Renzo, A. Zappone, M. Debbah, M.-S. Alouini, C. Yuen, J. de Rosny, and S. Tretyakov, "Smart radio environments empowered by reconfigurable intelligent surfaces: How it works, state of research, and the road ahead," *IEEE Journal on Selected Areas in Communications*, vol. 38, no. 11, pp. 2450–2525, 2020.
- [2] C. Pan, H. Ren, K. Wang, J. F. Kolb, M. ElKashlan, M. Chen, M. Di Renzo, Y. Hao, J. Wang, A. L. Swindlehurst, X. You, and L. Hanzo, "Reconfigurable intelligent surfaces for 6g systems: Principles, applications, and research directions," *IEEE Communications Magazine*, vol. 59, no. 6, pp. 14–20, 2021.
- [3] S. Zhang and R. Zhang, "Capacity characterization for intelligent reflecting surface aided mimo communication," *IEEE Journal on Selected Areas in Communications*, vol. 38, no. 8, pp. 1823–1838, 2020.
- [4] J. Zhang, J. Liu, S. Ma, C.-K. Wen, and S. Jin, "Large system achievable rate analysis of ris-assisted mimo wireless communication with statistical csit," *IEEE Transactions on Wireless Communications*, vol. 20, no. 9, pp. 5572–5585, 2021.
- [5] K. Xu, J. Zhang, X. Yang, S. Ma, and G. Yang, "On the sum-rate of ris-assisted mimo multiple-access channels over spatially correlated rician fading," *IEEE Transactions on Communications*, vol. 69, no. 12, pp. 8228–8241, 2021.
- [6] K. Zhi, C. Pan, H. Ren, and K. Wang, "Power scaling law analysis and phase shift optimization of ris-aided massive mimo systems with statistical csi," *IEEE Transactions on Communications*, vol. 70, no. 5, pp. 3558–3574, 2022.
- [7] Z. Peng, X. Chen, C. Pan, M. ElKashlan, and J. Wang, "Performance analysis and optimization for ris-assisted multi-user massive mimo systems with imperfect hardware," *IEEE Transactions on Vehicular Technology*, vol. 71, no. 11, pp. 11 786–11 802, 2022.
- [8] J. Dai, F. Zhu, C. Pan, H. Ren, and K. Wang, "Statistical csi-based transmission design for reconfigurable intelligent surface-aided massive mimo systems with hardware impairments," *IEEE Wireless Communications Letters*, vol. 11, no. 1, pp. 38–42, 2022.
- [9] K. Zhi, C. Pan, H. Ren, and K. Wang, "Ergodic rate analysis of reconfigurable intelligent surface-aided massive mimo systems with zf detectors," *IEEE Communications Letters*, vol. 26, no. 2, pp. 264–268, 2022.
- [10] K. Zhi, C. Pan, G. Zhou, H. Ren, M. ElKashlan, and R. Schober, "Is ris-aided massive mimo promising with zf detectors and imperfect csi?" *IEEE Journal on Selected Areas in Communications*, vol. 40, no. 10, pp. 3010–3026, 2022.
- [11] K. Zhi, C. Pan, H. Ren, and K. Wang, "Statistical csi-based design for reconfigurable intelligent surface-aided massive mimo systems with direct links," *IEEE Wireless Communications Letters*, vol. 10, no. 5, pp. 1128–1132, 2021.
- [12] A. Papazafeiropoulos, C. Pan, P. Kourtessis, S. Chatzinotas, and J. M. Senior, "Intelligent reflecting surface-assisted mu-miso systems with imperfect hardware: Channel estimation and beamforming design," *IEEE Transactions on Wireless Communications*, vol. 21, no. 3, pp. 2077–2092, 2022.
- [13] M. A. Mosleh, F. H  liot, and R. Tafazolli, "Ergodic capacity analysis of reconfigurable intelligent surface assisted mimo systems over rayleigh-rician channels," *IEEE Communications Letters*, pp. 1–1, 2022.
- [14] H. Guo, Y.-C. Liang, J. Chen, and E. G. Larsson, "Weighted sum-rate maximization for reconfigurable intelligent surface aided wireless networks," *IEEE Transactions on Wireless Communications*, vol. 19, no. 5, pp. 3064–3076, 2020.
- [15] R. Long, Y.-C. Liang, Y. Pei, and E. G. Larsson, "Active reconfigurable intelligent surface-aided wireless communications," *IEEE Transactions on Wireless Communications*, vol. 20, no. 8, pp. 4962–4975, 2021.
- [16] K. Zhi, C. Pan, H. Ren, K. K. Chai, and M. ElKashlan, "Active ris versus passive ris: Which is superior with the same power budget?" *IEEE Communications Letters*, vol. 26, no. 5, pp. 1150–1154, 2022.
- [17] M. H. Khoshafa, T. M. N. Ngatched, M. H. Ahmed, and A. R. Ndjiongue, "Active reconfigurable intelligent surfaces-aided wireless communication system," *IEEE Communications Letters*, vol. 25, no. 11, pp. 3699–3703, 2021.

- [18] K. Liu, Z. Zhang, L. Dai, S. Xu, and F. Yang, "Active reconfigurable intelligent surface: Fully-connected or sub-connected?" *IEEE Communications Letters*, vol. 26, no. 1, pp. 167–171, 2022.
- [19] Y. Ma, M. Li, Y. Liu, Q. Wu, and Q. Liu, "Active reconfigurable intelligent surface for energy efficiency in mu-miso systems," *IEEE Transactions on Vehicular Technology*, pp. 1–6, 2022.
- [20] B. Lyu, P. Ramezani, D. T. Hoang, S. Gong, Z. Yang, and A. Jamalipour, "Optimized energy and information relaying in self-sustainable ired-empowered wpcn," *IEEE Transactions on Communications*, vol. 69, no. 1, pp. 619–633, 2021.
- [21] Y. Zou, Y. Long, S. Gong, D. T. Hoang, W. Liu, W. Cheng, and D. Niyato, "Robust beamforming optimization for self-sustainable intelligent reflecting surface assisted wireless networks," *IEEE Transactions on Cognitive Communications and Networking*, vol. 8, no. 2, pp. 856–870, 2022.
- [22] Z. Chu, P. Xiao, D. Mi, W. Hao, M. Khalily, and L.-L. Yang, "A novel transmission policy for intelligent reflecting surface assisted wireless powered sensor networks," *IEEE Journal of Selected Topics in Signal Processing*, vol. 15, no. 5, pp. 1143–1158, 2021.
- [23] H. Ma, H. Zhang, W. Zhang, and V. C. M. Leung, "Beamforming optimization for reconfigurable intelligent surface with power splitting aided broadcasting networks," *IEEE Transactions on Vehicular Technology*, pp. 1–6, 2022.
- [24] W. Jaafar, L. Bariah, S. Muhaidat, and H. Yanikomeroglu, "Time-switching and phase-shifting control for ired-assisted swipt communications," *IEEE Wireless Communications Letters*, vol. 11, no. 8, pp. 1728–1732, 2022.
- [25] A. Wyner, "The wire-tap channel," *Bell Syst. Tech. J.*, vol. 54, no. 8, pp. 1355–1387, Oct. 1975.
- [26] P. K. Gopala, L. Lai, and H. El Gamal, "On the secrecy capacity of fading channels," *IEEE Trans. Inf. Theory*, vol. 54, no. 10, pp. 4687–4698, Oct. 2008.
- [27] W. Shi, Q. Wu, F. Xiao, F. Shu, and J. Wang, "Secrecy throughput maximization for ired-aided mimo wireless powered communication networks," *IEEE Transactions on Communications*, vol. 70, no. 11, pp. 7520–7535, 2022.
- [28] L. Dong, H.-M. Wang, and J. Bai, "Active reconfigurable intelligent surface aided secure transmission," *IEEE Transactions on Vehicular Technology*, vol. 71, no. 2, pp. 2181–2186, 2022.
- [29] H. Guo, Z. Yang, Y. Zou, B. Lyu, Y. Jiang, and L. Hanzo, "Joint reconfigurable intelligent surface location and passive beamforming optimization for maximizing the secrecy-rate," *IEEE Transactions on Vehicular Technology*, pp. 1–13, 2022.
- [30] J. Luo, F. Wang, S. Wang, H. Wang, and D. Wang, "Reconfigurable intelligent surface: Reflection design against passive eavesdropping," *IEEE Transactions on Wireless Communications*, vol. 20, no. 5, pp. 3350–3364, 2021.
- [31] J. Bai, H.-M. Wang, and P. Liu, "Robust ired-aided secrecy transmission with location optimization," *IEEE Transactions on Communications*, vol. 70, no. 9, pp. 6149–6163, 2022.
- [32] W. Lv, J. Bai, Q. Yan, and H.-M. Wang, "Rid-assisted green secure communications: Active rid or passive rid?" *IEEE Wireless Communications Letters*, pp. 1–1, 2022.
- [33] P. Xu, G. Chen, G. Pan, and M. D. Renzo, "Ergodic secrecy rate of rid-assisted communication systems in the presence of discrete phase shifts and multiple eavesdroppers," *IEEE Wireless Communications Letters*, vol. 10, no. 3, pp. 629–633, 2021.